Inorganic Chemistry

Article

pubs.acs.org/IC

Preparation of a Diphosphine with Persistent Phosphinyl Radical Character in Solution: Characterization, Reactivity with O_2, S_8, Se, Te, and P_4, and Electronic Structure Calculations

Nick A. Giffin,[†] Arthur D. Hendsbee,[†] Tracey L. Roemmele,[‡] Michael D. Lumsden,[§] Cory C. Pye,[†] and Jason D. Masuda*,[†]

[†]The Maritimes Centre for Green Chemistry and the Department of Chemistry, Saint Mary's University, Halifax, Nova Scotia, Canada B3H 3C3

[‡]Department of Chemistry and Biochemistry, University of Lethbridge, Lethbridge, Alberta, Canada T1K 3M4

[§]Nuclear Magnetic Resonance Research Resource (NMR-3), Department of Chemistry, Dalhousie University, Halifax, Nova Scotia, Canada B3H 4J3

Supporting Information

ABSTRACT: A new, easily synthesized diphosphine based on a heterocyclic 1,3,2-diazaphospholidine framework has been prepared. Due to the large, sterically encumbering Dipp groups (Dipp = 2,6-diisopropylphenyl) on the heterocyclic ring, the diphosphine undergoes homolytic cleavage of the P−P bond in solution to form two phosphinyl radicals. The diphosphine has been reacted with O_2, S_8, Se, Te, and P_4, giving products that involve insertion of elements between the P−P bond to yield the related phosphinic acid anhydride, sulfide/disulfide, selenide, telluride, and a butterfly-type perphospha-bicyclo-butadiene structure with a *trans,trans*-geometry. All molecules have been characterized by multinuclear NMR spectroscopy, elemental analysis, and single-crystal X-ray crystallography. Variable-temperature EPR spectroscopy was utilized to study the nature of the phosphinyl radical in solution. Electronic structure calculations were performed on a number of systems from the parent diphosphine $[H_2P]_2$ to amino-substituted $[(H_2N)_2P]_2$ and cyclic amino-substituted $[(H_2C)_2(NH)_2P]_2$; then, bulky substituents (Ph or Dipp) were attached to the cyclic amino systems. Calculations on the isolated diphosphine at the B3LYP/6-31+G* level show that the homolytic cleavage of the P−P bond to form two phosphinyl radicals is favored over the diphosphine by ∼11 kJ/mol. Furthermore, there is a significant amount of relaxation energy stored in the ligands (52.3 kJ/mol), providing a major driving force behind the homolytic cleavage of the central P−P bond.

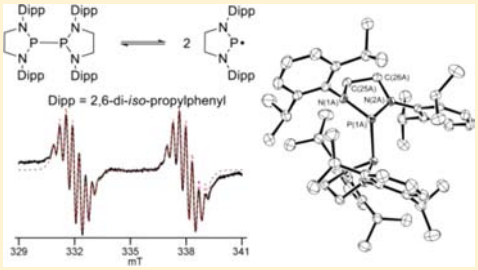

1. INTRODUCTION

First-row main group free radicals have been present in the literature since the early 19th century. The triphenylmethyl or Gomberg radical exemplifies these early radicals, and was first reported in 1900. On the basis of elemental analysis executed in a bayonet tube, Gomberg proposed this compound as a trivalent carbon species, the first low-valent main group compound in the literature.[1] The characterization of radicals centered on heavier main group elements such as phosphorus was slower to develop.[2] Preliminary forays toward the characterization of radical-containing phosphorus species were developed in the synthesis of organic species, facilitated by phosphorus-centered radical mechanisms.[3,4] However, definitive spectroscopic evidence was not presented until 1969 with the reaction of a trialkyl-phosphorus center with the *tert*-butoxyl radical yielding the first unequivocal evidence of an observable phosphorus-centered molecule containing an unpaired electron.[5] Several persistent or stable phosphorus-centered radicals have since been described within the subclasses of phosphorus-centered radicals, including phosphinyl ($\bullet PR_2$),[6−16] phosphonyl ($\bullet POR_2$),[17] phosphoniumyl $[\bullet PR_3]^+$,[18] and phosphidyl radical anions $[\bullet PR_3]^-$,[18] which have been included in the content of recent reviews.[19−21]

Two general approaches can be employed to stabilize molecules containing a radical electron(s): (1) increasing steric bulk surrounding the radical center, providing kinetic and thermodynamic stabilization; this can prevent unwanted reactivity or dimerization; and (2) placing radical centers adjacent to electronegative atoms, providing electronic stabilization of the singly occupied molecular orbital (SOMO) by dispersing the radical character through a conjugated system. Using these approaches, notable recent advances in structurally characterized persistent phosphorus-centered radicals include recent tungsten-supported, **A**,[22] and vanadium-supported structures, **B**,[13] as well as an air-tolerant diphosphacyclobuten-4-yl radical, **C**.[23,24] Recent isolation of carbene-stabilized phosphinyl radical cation **D**,[14] diphosphine **E**,[25] and phosphorus mononitride **F**[26] radical cations, as well as imididazolidin-2-iminato **G**[15] and vanadium-iminato **H**[15]

Received: August 10, 2012
Published: October 25, 2012

   dx.doi.org/10.1021/ic301758k | Inorg. Chem. 2012, 51, 11837−11850

phosphorus-centered radicals are noted in the literature. Finally, Ishida and co-workers were able to isolate the alkyl-substituted phosphinyl **I**,[16] which is stable in both solution and solid state (see Chart 1 for compounds **A**–**I**).

Chart 1. Compounds A–I; Dipp = 2,6-diisopropylphenyl; Mes* = 2,4,6-tri*tert*butylphenyl; R = [3,5-$Me_2C_6H_3$)(neopentyl)N]

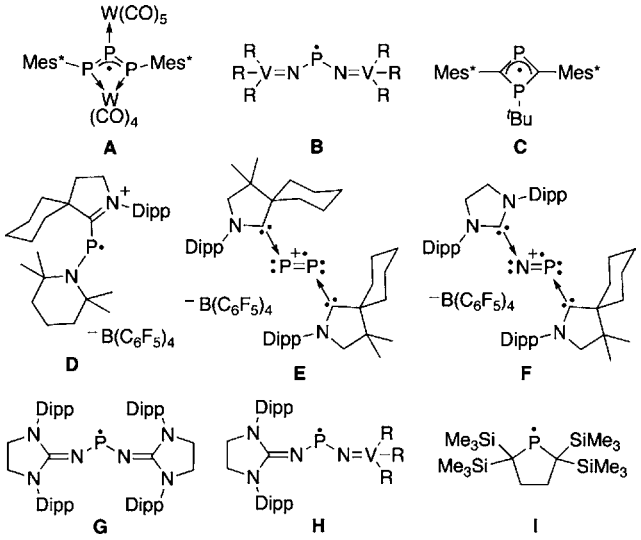

From a synthetic standpoint, early phosphinyl radicals were generated photolytically in the presence of electron-rich olefins and were characterized using electroparamagnetic resonance spectroscopy (EPR).[5−7,27] However, facile generation of phosphinyl species is also possible through homolytic cleavage of a weak or strained, phosphorus−phosphorus bond via sterically congested diphosphine molecules.

A particularly noteworthy example of such radical formation involves the diphosphine **J**, known in the literature as a molecular "jack-in-the-box".[8,9] The moniker attributed to this molecule is a product of the strained rotation of the bis(trimethylsilyl)methyl ligands described as "molecular springs" which upon solvation undergo an energetically favorable dissociative relaxation to the monomeric radical. This is supported by density functional theory (DFT) calculations indicating an overall exothermic dissociation process while undergoing solvation or sublimation.[28−30] The steric and electronic interactions produce an elongated (2.3103(7) Å) bond in the solid state that is primed for dissociation. Later, a report by Lappert et al. reexamined the phosphinyl $[(Me_3Si)_2N][(^iPr)_2N]P\bullet$[7] using gas-phase electron diffraction and isolated the related diphosphine **K**, showing that homolytic cleavage of the P−P bond occurred in heated hexane solutions. Recently, Wright et al. produced a sterically hindered, N-heterocyclic based, P−P dimers **L** that undergo dissociation to persistent 7π-radicals as determined by EPR spectroscopy.[31] Subsequently, Gudat et al. completed a comprehensive synthetic and spectroscopic study on **L** (R = Dipp).[32] These sterically bulky diamino-diphosphines are of interest as they satisfy both the electronic and kinetic requirements for stabilizing phosphinyl species in solution (see Chart 2).

In this work, we report the synthesis and characterization of a new, sterically bulky diphosphine, $[(H_2C)_2(NDipp)_2P]_2$ **1**, that undergoes homolytic cleavage of the phosphorus−phosphorus bond upon dissolution in common solvents at room temperature. This diphosphine is easily synthetically accessible, repeatable, and can be prepared in gram-scale quantities with decent isolated yields. EPR spectroscopy highlights that the diphosphine exists in solution below room temperature. A computational study has been paired with the synthetic work and indicates that the P−P bond cleavage is favorable and manifests itself in an energetically exothermic dissociative relaxation process as a result of the extreme distortion in the ligand that is chelated to the phosphorus center. In addition, calculations on model systems $([H_2P]_2$, $[(H_2N)_2P]_2$, $[(H_2C)_2(NH)_2P]_2$, and $[(H_2C)_2(NPh)_2P]_2$ have been analyzed and compared. Finally, reactions of the diphosphine/phosphinyl system with dioxygen, elemental sulfur (S_8), elemental selenium, elemental tellurium, and white phosphorus (P_4) have been investigated and the products fully characterized.

Chart 2. Compounds J–L

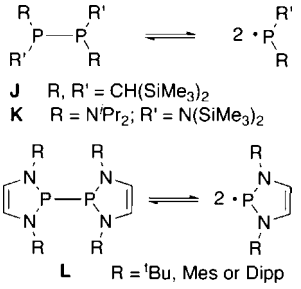

2. EXPERIMENTAL SECTION

2.1. General Synthetic Procedures. All preparations were done under an atmosphere of dry, O_2-free N_2, employing both Schlenk line techniques and an mBraun Labmaster SP inert atmosphere glovebox. Toluene, pentane, and tetrahydrofuran were purified employing a Grubbs'-type solvent purification system manufactured by Innovative Technology. Elemental analysis was carried out at the Saint Mary's University Center for Environmental Analysis and Remediation (CEAR) on a PerkinElmer 2400 series II CHN analyzer or by Canadian Microanalytical Service Ltd. Melting points were recorded on an Electrothermal MEL-Temp 3.0 using glass capillaries with samples prepared and sealed under inert conditions. Hyflo Super Cel (Celite) was purchased from Aldrich Chemical Co. and dried for 24 h in an oven prior to use. Molecular sieves (4 Å) were purchased from Aldrich Chemical Co. and dried overnight at 140 °C under vacuum. Crude white phosphorus (Aldrich) was removed from water and dried under vacuum, dissolved in CS_2, and then passed through a cannula fitted with a glass fiber filter. The CS_2 was removed under reduced pressure, and the resulting white solid was stored in a glovebox freezer (−35 °C). 2-Chloro-1,3-bis(2,6-diisopropylphenyl)-1,3,2-diazaphospholidine **2** was prepared according to an updated literature procedure[33] of the original method.[34] The crystal structure of **2** was obtained and is included in the Supporting Information (Figure S1).

2.2. Preparation of $[(H_2C)_2(NDipp)_2P]_2$ (1). In a 20 mL scintillation vial, 1.7 g (13 mmol) of naphthalene was dissolved in 10 mL of tetrahydrofuran and rapidly stirred with a Teflon-coated stir bar. Then 0.26 g (11 mmol) of Na^0 was added in small, freshly divided pieces. The resultant forest-green solution was allowed to stir for 30 min at which point 5.0 g (11 mmol) of chlorophosphine **2** in 10 mL of tetrahydrofuran was added dropwise. The resulting bright-orange reaction mixture was allowed to stir overnight. Volatiles were removed under vacuum, and the remaining solids were extracted with pentane and filtered through a pad of diatomaceous earth on a fritted funnel. The pentane was removed *in vacuo*. The naphthalene was removed *via* sublimation *in vacuo* at 60 °C for approximately 8 h. The resultant orange solid was crystallized from a concentrated, room-temperature solution of pentane cooled to −35 °C over several days, yielding 3.4 g

dx.doi.org/10.1021/ic301758k | *Inorg. Chem.* 2012, 51, 11837−11850

(4.2 mmol, 74% recovery) of **1** in two crops of crystals. Low recovered yields can be attributed to the extreme solubility of the diphosphine in most compatible solvents (e.g., THF, pentane, toluene). Melting point: 219−220 °C. $^{31}P\{^1H\}$ (101.2 MHz, C_6D_6): δ = 143.5 ppm. ^1H NMR (500 MHz, toluene-d_8, 268 K): δ = 7.21−7.13 (m, 8H, Ar−H), 7.00−6.94 (m, 4H, Ar−H), 4.18 (br m, 2H, CH/CH_2), 4.01 (br m, 2H, CH/CH_2), 3.64−3.57 (br m, 4H, CH/CH_2), 3.44 (br m, 2H, CH/CH_2), 3.25 (br m, 2H, CH/CH_2), 2.94 (br m, 2H, CH/CH_2), 2.83 (br m, 2H, CH/CH_2), 1.47−1.42 (br m, 12H, CH_3), 1.30−1.14 (br m, 27H, CH_3), 0.93−0.87 (br m, 3H, CH_3), 0.38 (br s, 6H, CH_3). $^{13}C\{^1H\}$ NMR (125.7 MHz, C_6D_6): δ = 149.15, 148.81, 126.40, 124.79, 124.37, 57.72, 54.55, 30.46, 29.30, 28.45, 24.67, 23.06, 14.62. Anal. Calc for $C_{52}H_{76}N_4P_2$: C, 76.25; H, 9.35; N, 6.84. Found: C, 75.99; H, 9.72; N, 6.73.

2.3. Preparation of ((H$_2$C)$_2$(NDipp)$_2$P(O))-O-(P(O)-(NDipp)$_2$(CH$_2$)$_2$) (3). In a J-Young style NMR tube, 100 mg (0.122 mmol) of **1** was dissolved in 0.6 mL of deuterated toluene to give an orange−red solution. The sample was degassed using three freeze−pump−thaw cycles at which point oxygen gas was introduced at approximately one atmosphere of pressure. The tube was sealed and shaken vigorously. After 30 min the sample had lost all color, and $^{31}P\{^1H\}$ NMR indicated virtually quantitative conversion to **3**. X-ray quality, colorless blocklike crystals (55 mg, 6.3 mmol) were grown through slow evaporation of toluene at ambient temperatures. Isolated Yield: 52%. Melting point: 190−192 °C. $^{31}P\{^1H\}$ NMR (101.2 MHz, C_6D_6): δ = 4.4 ppm. ^1H NMR (500 MHz, C_6D_6): δ = 7.30−7.16 (m, 6H, Ar−H), 7.14−6.97 (m, 6H, Ar−H), 4.04 (sept, 2H, CH, $^3J_{H-H}$ = 7 Hz), 3.87 (sept, 1H, CH, $^3J_{H-H}$ = 7 Hz), 3.81 (sept, 1H, CH, $^3J_{H-H}$ = 7 Hz), 3.69 (sept, 1H, CH, $^3J_{H-H}$ = 7 Hz), 3.59 (q, 2H, CH_2, $^3J_{H-H}$ = 7 Hz), 3.52−3.21 (m, 6H, CH/CH_2), 3.13 (sept, 1H, CH, $^3J_{H-H}$ = 7 Hz), 3.07 (s, 0.5H, residual solvent), 2.95−2.88 (m, 2H, CH/CH_2), 1.63 (d, 3H, CH_3, $^3J_{H-H}$ = 7 Hz), 1.56 (d, 3H, CH_3, $^3J_{H-H}$ = 7 Hz), 1.47 (d, 3H, CH_3, $^3J_{H-H}$ = 7 Hz), 1.40 (d, 2H, CH_3, $^3J_{H-H}$ = 7 Hz), 1.37−1.25 (m, 6H, CH_3), 1.23 (d, 3H, CH_3, $^3J_{H-H}$ = 7 Hz), 1.21−1.04 (overlapping doublets, 21H, CH_3), 1.04 (d, 3H, CH_3, $^3J_{H-H}$ = 7 Hz), 0.62 (d, 3H, CH_3, $^3J_{H-H}$ = 7 Hz). $^{13}C\{^1H\}$ NMR (75.4 MHz, C_6D_6): δ = 150.66, 150.27, 136.49, 135.90, 124.53, 124.18, 51.12, 49.16, 29.58, 29.44, 29.23, 28.83, 28.65, 28.45, 27.58, 27.27, 26.77, 26.43, 26.32, 25.96, 25.82, 25.71, 25.36, 25.24, 25.02, 24.79, 24.62, 24.49. Anal. Calc for $C_{52}H_{76}N_4P_2O_3$: C, 72.03; H, 8.83; N, 6.46. Found: C, 71.19; H, 8.86; N, 6.47.

2.4. Preparation of ((H$_2$C)$_2$(NDipp)$_2$P)-S$_x$-(P(NDipp)$_2$(CH$_2$)$_2$); *x* = 1 (10%), 2 (90%) (4). In a 20 mL scintillation vial, 100 mg (0.122 mmol) of **1** was dissolved in 10 mL of toluene and rapidly stirred with a Teflon-coated stir bar. Then 31.2 mg (0. 122 mmol) of S_8 was added as a partially dissolved suspension in 2 mL of toluene. The resultant pale-yellow solution was allowed to stir for 30 min at which point the solution transitioned to colorless. The solution was filtered through a pad of Celite and crystallized via slow evaporation of the solvent at ambient temperatures, yielding 85 mg of X-ray quality, colorless crystals. Melting point: 175−177 °C. $^{31}P\{^1H\}$ NMR (101.2 MHz, C_6D_6): δ = 154.4 (P−S−S−P), 136.0 (P−S−P) ppm. ^1H (500 MHz, C_6D_6) δ = 7.23−7.17 (m, 4H, Ar−H), 7.14−7.01 (m, 8H, Ar−H), 3.40 (sept, 2H, CH, $^3J_{H-H}$ = 7 Hz), 3.87−3.68 (m, 4H, CH_2/CH), 3.64 (q, 1H, CH_2, $^3J_{H-H}$ = 7 Hz), 3.31−3.52 (m, 4H, CH, $^3J_{H-H}$ = 7 Hz), 3.25 (sept, 1H, CH, $^3J_{H-H}$ = 7 Hz), 3.04−3.09 (m, 4H, CH_2), 1.56 (d, 3H, CH_3, $^3J_{H-H}$ = 7 Hz), 1.45 (d, 3H, CH_3, $^3J_{H-H}$ = 7 Hz), 1.35 (br m, 3H, CH_3), 1.24−1.30 (m, 6H, CH_3), 1.21 (d, 3H, CH_3, $^3J_{H-H}$ = 7 Hz), 1.20 (d, 3H, CH_3, $^3J_{H-H}$ = 7 Hz), 1.17 (d, 6H, CH_3, $^3J_{H-H}$ = 7 Hz), 1.15 (d, 6H, CH_3, $^3J_{H-H}$ = 7 Hz), 1.11−1.07 (m, 9H, CH_3), 0.96−0.84 (m, 6H, CH_3). $^{13}C\{^1H\}$ (75.4 MHz, C_6D_6): δ = 150.36, 149.49, 124.81, 124.29, 123.78, 123.53, 54.53, 50.01, 29.83, 28.69, 25.63, 25.43, 24.97, 24.58, 24.30, 24.03, 23.56. Anal. Calc for 90% $C_{52}H_{76}N_4P_2S$·10% $C_{52}H_{76}N_4P_2S_2$·1/2C_7H_8: C, 73.20; H, 8.96; N, 6.52. Found: C, 73.03; H, 9.46; N, 5.98.

2.5. Preparation of ((H$_2$C)$_2$(NDipp)$_2$P)-Se-(P(NDipp)$_2$(CH$_2$)$_2$) (5). In a 20 mL scintillation vial, 100 mg (0.122 mmol) of **1** was dissolved in 5 mL of THF and rapidly stirred with a Teflon-coated stir bar. Then 9.6 mg (0.122 mmol) of Se^0 was added as a suspension in 5 mL of THF. The orange solution with gray precipitate was allowed to stir overnight at which point the solution transitioned from orange in color to colorless. The solvent was removed *in vacuo*, dissolved in toluene, filtered through a pad of diatomaceous earth to remove excess selenium metal, and crystallized *via* slow evaporation of the solvent at ambient temperatures, yielding 83 mg of X-ray quality, colorless crystals. Isolated yield: 76%. Melting point: 182−185 °C. $^{31}P\{^1H\}$ NMR (121.5 MHz, C_6D_6): δ = 160.01 (sat d, $^1J_{P-Se}$ = 141 Hz). ^1H NMR (300 MHz, C_6D_6): δ = 7.18 (2H, Ar-*H*), 7.13 (m, 2H, Ar-*H*), 7.06−7.03 (m, 8H, Ar-*H*), 3.79−3.64 (m, 8H, *CH*/CH_2), 3.57 (m, residual THF), 3.41 (sept, 4H, CH, $^3J_{H-H}$ = 7 Hz), 3.11−3.06 (m, 4H, CH_2), 1.40 (m, residual THF), 1.19−1.16 (overlapping doublets, 24H, CH_3), 1.07−1.03 (overlapping doublets, 24H, CH_3). $^{13}C\{^1H\}$ NMR (75.4 MHz, C_6D_6): δ = 149.60, 147.93, 138.08, 127.34, 124.89, 124.05, 67.79 (residual THF), 55.24, 28.86, 28.80, 28.73, 25.96, 25.79, 25.57, 24.54, 24.22. Anal. Calc for $C_{52}H_{76}N_4P_2Se$: C, 69.54; H, 8.53; N, 6.24. Found: C, 69.59; H, 8.65; N, 6.15.

2.6. Preparation of ((H$_2$C)$_2$(NDipp)$_2$P)-Te-(P(NDipp)$_2$(CH$_2$)$_2$) (7). In a 20 mL scintillation vial, 100 mg (0.122 mmol) of **1** was dissolved in 5 mL of THF and rapidly stirred with a Teflon-coated stir bar. Then 78 mg (0.61 mmol, 5 equiv) of Te^0 was added as a suspension in 5 mL of THF. The orange solution with gray/black precipitate was allowed to stir overnight at which point the solution transitions to yellow in color. THF was removed *in vacuo*. The solid was dissolved in toluene, filtered through a pad of diatomaceous earth to remove excess tellurium metal and crystallized *via* slow evaporation of the solvent at ambient temperatures yielding 95 mg of X-ray quality, colorless crystals of **7**. Isolated Yield: 82% Melting point: 196−199 °C. $^{31}P\{^1H\}$ NMR (121.5 MHz, C_6D_6): δ = 177.07 (sat d, $^1J_{P-Te}$ = 278 Hz) ^1H NMR (300 MHz, C_6D_6): δ = 7.18−7.04 (m, 12H, Ar-*H*), 7.01 (m, 5H, Ar-*H* residual toluene), 3.66 (q, 4H, CH_2, $^3J_{H-H}$ = 7 Hz), 3.59 (sept, 4H, *CH*, $^3J_{H-H}$ = 7 Hz), 3.43 (sept, 4H, *CH*, $^3J_{H-H}$ = 7 Hz), 3.12 (q, 4H, CH_2, $^3J_{H-H}$ = 7 Hz), 2.11 (s, 3H, CH_3, residual toluene), 1.89 (d, 12H, CH_3, $^3J_{H-H}$ = 7 Hz), 1.14 (d, 12H, CH_3, $^3J_{H-H}$ = 7 Hz), 1.08 (d, 12H, CH_3, $^3J_{H-H}$ = 7 Hz), 1.00 (d, 12H, CH_3, $^3J_{H-H}$ = 7 Hz). $^{13}C\{^1H\}$ NMR (75.4 MHz, C_6D_6): δ = 149.53, 148.07, 129.29, 127.43, 125.17, 124.02, 55.07, 29.00, 28.66, 25.91, 25.47, 25.40, 24.38. Anal. Calc for $C_{52}H_{76}N_4P_2Te$·C_7H_8: C, 68.21; H, 8.15; N, 5.39. Found: C, 68.52; H, 8.22; N, 5.69.

2.7. Preparation of ((H$_2$C)$_2$(NDipp)$_2$P)P$_4$(P(NDipp)$_2$(CH$_2$)$_2$) (8). In a J-Young style NMR tube, 66 mg (0.081 mmol) of **1** was combined with a solution of P_4 (10 mg, 0.081 mmol) in 0.6 mL of deuterated toluene. Over a 60 min time period the orange−red solution turned yellow and $^{31}P\{^1H\}$ NMR spectroscopy revealed quantitative conversion to **8**. X-ray quality, yellow-gold block-like single crystals were grown from toluene at −35 °C over several days. Melting point: 237−240 °C. $^{31}P\{^1H\}$NMR: Modeling of the P_6 system core as AA′MM′X_2 yielded (δ): A = 160.7 ppm, M = −108.2 ppm, X = −349.5 ppm, J_{AM} = $J_{A'M'}$ = −214.9 Hz, J_{MX} = $J_{M'X}$ = −152.8 Hz, J_{AX} = $J_{A'X}$ = +99.2 Hz, $J_{MM'}$ = +101.1 Hz, $J_{AM'}$ = $J_{A'M}$ = −61.2 Hz. See section 2.6 for simulation details. ^1H NMR (500 MHz, C_6D_6): δ = 6.91−7.08 (12H, Ar−H), 3.77 (sept, 4H, *CH*CH_3, $^3J_{H-H}$ = 7 Hz), 3.60 (m, 4H, CH_2), 3.34 (sept, 4H, *CH*CH_3, $^3J_{H-H}$ = 7 Hz), 2.99 (m, 4H, CH_2), 2.07 (s, 1.7H, residual solvent), 1.46 (d, 12H, CH_3, $^3J_{H-H}$ = 7 Hz), 1.15 (d, 12H, CH_3, $^3J_{H-H}$ = 7 Hz), 1.10 (d, 12H, CH_3, $^3J_{H-H}$ = 7 Hz), 1.06 (d, 12H, CH_3, $^3J_{H-H}$ = 7 Hz). $^{13}C\{^1H\}$ NMR (125.7 MHz, C_6D_6): δ = 150.01, 148.65, 138.29, 138.19, 125.14, 125.04, 65.77, 55.95, 53.27, 30.11, 29.47, 26.51, 26.07, 25.97, 24.99, 24.80. Anal. Calc for $C_{49}H_{70}N_4P_6$·1/2C_7H_8: C, 67.39; H, 8.15; N, 5.66. Found: C, 67.32; H, 7.72; N, 5.49.

2.8. NMR Spectroscopy. NMR spectra were recorded on Bruker-Avance 500 MHz, Bruker-Avance 300 MHz, AC-250 MHz, and Varian EM360 60 MHz spectrometers. Trace amounts of protonated solvent were used as internal references for ^1H NMR spectra and were referenced relative to tetramethylsilane. The deuterated solvent was used as an internal reference for $^{13}C\{^1H\}$ NMR spectra (referenced relative to tetramethylsilane), whereas ^{31}P NMR spectra were referenced to external 85% H_3PO_4. Coupling constants are reported as absolute values.

In order to simulate the complex $^{31}P\{^1H\}$ spectrum in **8**, experimental data were obtained at three different external magnetic

Table 1. Crystallographic Data for Compounds 1−5, 7, and 8

cmpd	1	2	3	4	5	7	8
chemical formula	$C_{52}H_{76}N_4P_2$	$C_{26}H_{38}ClN_2P$	$C_{52}H_{76}N_4O_3P_2$	$C_{52}H_{76}N_4P_2S_{1.87}$	$C_{52}H_{76}N_4P_2Se$	$C_{125}H_{176}N_8P_4Te_2$	$C_{52}H_{76}N_4P_6$
formula mass	819.11	445.00	867.11	879.06	898.07	2169.82	942.99
cryst syst	orthorhombic	monoclinic	monoclinic	triclinic	triclinic	triclinic	tetragonal
a/Å	12.3916(15)	12.017(5)	16.186(4)	12.108(6)	20.648(5)	12.5708(10)	12.954(3)
b/Å	17.744(2)	16.597(7)	17.938(4)	21.507(11)	23.568(6)	13.2461(10)	12.954(3)
c/Å	24.391(3)	12.765(5)	17.738(4)	21.647(11)	24.274(6)	20.3636(16)	35.031(12)
α/deg	90.00	90.00	90.00	65.859(7)	67.160(3)	83.0370(10)	90.00
β/deg	90.00	97.632(5)	101.922(3)	89.905(7)	84.262(3)	77.0790(10)	90.00
γ/deg	90.00	90.00	90.00	86.889(7)	83.823(3)	70.3580(10)	90.00
unit cell vol/Å^3	5362.8(11)	2523.3(17)	5039(2)	5135(4)	10801(5)	3108.7(4)	5878.4(28)
temp/K	296(2)	130(2)	135(2)	150(2)	130(2)	150(2)	130(2)
space group	*Pccn*	*P*2(1)/*c*	*P*2(1)/*n*	$P\bar{1}$	$P\bar{1}$	$P\bar{1}$	*P*4(1)2(1)2
Z	4	4	4	4	8	1	4
radiation type	Mo Kα	Mo Kα	Mo Kα	Mo Kα	Mo Kα	Mo Kα	Mo Kα
abs coeff μ/mm^{-1}	0.115	0.230	0.130	0.198	0.789	0.568	0.217
reflns	40991	26400	48892	34578	70274	20865	71003
independent reflns	6578	4957	8872	17760	37157	17209	7296
R_{int}	0.0804	0.0591	0.0768	0.0723	0.0763	0.0319	0.0562
final R_1 ($I > 2\sigma(I)$)	0.0517	0.0398	0.0500	0.0670	0.0993	0.0507	0.0631
final $wR(F^2)$ ($I > 2\sigma(I)$)	0.1115	0.0891	0.1096	0.1454	0.2451	0.1076	0.1631
final R_1 (all data)	0.0929	0.0589	0.0875	0.1367	0.1588	0.0747	0.0720
final $wR(F^2)$ (all data)	0.1231	0.0981	0.1300	0.1867	0.2752	0.1205	0.1689
GOF on F^2	1.031	1.046	1.005	0.973	0.963	0.963	1.070

field strengths (11.7, 5.9, and 1.4 T corresponding to ^{31}P Larmor frequencies of 202.4, 101.2, and 24.3 MHz, respectively). Simulations were performed using the higher field data first, making use of connectivity information obtained via ^{31}P−^{31}P COSY experiments. The uniqueness of the solution was subsequently verified using the simulated parameters obtained at 11.7 T to calculate ^{31}P{^{1}H} spectra obtained at 5.9 and 1.4 T. The quality of the fits in all cases was also verified by examining the singular value decomposition matrix provided by gNMR. The absolute signs of P−P coupling constants were assigned by using the assumption that all ^1J(P−P) coupling constants are negative.[35] Letter designations in the phosphorus spin system have been assigned by calculating the ratio of the phosphorus chemical shift differences to the magnitude of the coupling constant, using a value of 10 as the threshold between a first- and second-order letter designation.

2.9. Electronic Structure Calculations. Calculations were performed using *Gaussian03*[36] or *Gaussian09*,[37] using a stepping-stone approach in which the geometries at the levels HF/STO-3G, HF/3-21G, HF/6-31G*, HF/6-31+G*, B3LYP/6-31G*, and B3LYP/6-31+G* were sequentially optimized using default specifications. After each level, a frequency calculation was performed to verify the nature of the stationary point. *Z*-matrix coordinates constrained to the appropriate symmetry were used for efficiency, as any problems would manifest themselves by an imaginary mode orthogonal to the spanned *Z*-matrix space. The Hessian was also evaluated at the starting STO-3G geometry to aid convergence. EPR hyperfine splitting (hfs) constants for **1** were calculated at the B3LYP/6-31+G* level of theory. For the potential energy scan calculations, the guess = mixed keyword was used to allow the ground-state singlet to be a diradicaloid, if necessary.

2.10. EPR Spectroscopy. X-band EPR spectra were recorded on a sample of **1** over temperatures of −20−39 °C using a Bruker EMX 113 spectrometer. The sample was prepared inside a glovebox, transferred into 4.0-mm EPR tube, and sealed prior to data collection. Hyperfine coupling constants were determined by spectral simulation using *Winsim* (version 0.98, 2002) software.[38]

2.11. X-ray Crystallography. Crystals of compounds **1**−**8** were mounted from Paratone-N oil in a nylon cryoloop or on a MiTeGen MicroMount. The data were collected on a Bruker D8 APEX II charge-coupled-device (CCD) diffractometer, with a KRYO-FLEX cooling device. The instrument was equipped with graphite-monochromated Mo Kα radiation (λ = 0.71073 Å), with MonoCap X-ray source optics. A hemisphere of data was collected using ω scans, with frame exposures of 5−30 s and 0.3° frame widths. Data collection and initial indexing and cell refinement were handled using APEX II software.[39] Frame integration, including Lorentz-polarization corrections, and final cell parameter calculations were carried out using *SAINT*+ software.[39] The data were corrected for absorption using the *SADABS* program.[39] The structures were solved using direct methods and difference Fourier techniques. Structure solution, refinement, and creation of publication materials were performed using *SHELXL*.[40] All hydrogen atom positions were idealized and rode on the atom to which they were attached. The final refinement included anisotropic temperature factors on all non-hydrogen atoms. Details of crystal data, data collection, and structure refinement are listed in Table 1. All figures were made using *ORTEP-3 for Windows*.[41] Additional details of the data collection and structure refinement and tables of bond lengths and angles are given in the Supporting Information.

3. RESULTS AND DISCUSSION

3.1. Synthesis and Characterization of Diphosphine. Diphosphine **1** is prepared from the known chlorophosphine **2** (see Scheme 1). Attempts to reduce the chlorophosphine **2** with Mg, Na, K, Li, were fruitless and only resulted in recovery of starting material. Reduction using sodium naphthalide in tetrahydrofuran at room temperature resulted in the formation of an orange-colored solution. Analysis of this solution by ^{31}P

Scheme 1. Preparation of diphosphine 1[a]

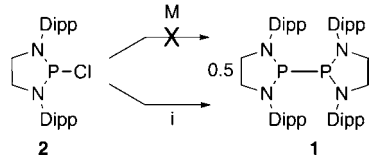

[a]Reagents and conditions: M = Li, Na, K, Mg, Zn in THF; i) Na + naphthalene in THF.

NMR revealed loss of the starting material (δ 154 ppm[33,34]) and the formation of a single new peak at δ 143 ppm. Filtration and removal of solvent and naphthalene by sublimation under vacuum gave an orange solid that was crystallized from pentane to give red−orange-colored blocks. Analysis of the ^{1}H NMR spectrum in benzene-d_6 or toluene-d_8 at room temperature revealed a number of broad peaks that were indicative of either a dynamic process occurring in solution or the presence of a radical species. Subsequent cooling of the toluene sample to −5 °C resulted in a significant sharpening of the peaks (Figure S2). There was no change in the ^{31}P NMR chemical shift at these temperatures. It should be noted that less sterically congested analogues (R = Mes or 2,6-dimethylphenyl) have been prepared in low yield by metathesis of $(H_2C)_2(NR)_2P$-PPh_2 to give tetraphenyldiphosphane and $[(H_2C)_2(NR)_2P]_2$.[42]

Analysis by single-crystal X-ray crystallography revealed the expected diphosphine **1** (Figure 1) in the orthorhombic space group *Pccn* with two-site disorder of the five-membered heterocyclic ring (94:6). The major disordered component of the structure features the typical eclipsed diphosphine structure (N1a−P1a−P1a−N1a dihedral = 7.14(18)°) with the chelating diamine ligands on each phosphorus atom forming the heterocycle. The P−P bond distance is 2.3207(9) Å and while significantly longer than a typical diphosphine such as tetraphenyldiphosphine (2.217(1) Å)[43] it is similar to other sterically encumbered diphosphines in the literature such as **J** (2.310(7) Å)[8,9] and **L** (R = Dipp 2.33 Å; R = Mes 2.324(2) Å).[31] In order to accommodate the large Dipp groups in the diphosphine molecule there are significant distortions to the ligand itself. For example, in chlorophosphine **2**, the nitrogen atoms are nearly planar (sum of angles 358.64 and 359.71°), whereas in **1**, although N2a is planar (sum of angles 359.82°), N1a has become pyramidal with a sum of angles of 353.36°. This bending of the Dipp group is manifested in the steric constrictions of the ligand and allows the Dipp group to fold into an open pocket of the other half of the diphosphine. Dipp ring C1−C6 attached to N2A is twisted from the mean plane of the heterocycle (P1A−N1A−C25A−C26A−N2A) by 61.89(5)°, and C1 lies 0.253(3) Å out of the mean heterocyclic plane (MHP). Dipp ring C7−C12 connected to N1A is orthogonal to the heterocyclic plane (89.93(5)°) but is significantly bent from the heterocycle with a C7−MHP distance of 1.0765(28) Å. This significant distortion of the ligand framework plays a strong role in the ability of the phosphinyl radical to form as this distortion has been calculated to have a relaxation energy of 52.3 kJ/mol at the B3LYP/6-31+G* level of theory (*vide infra*).

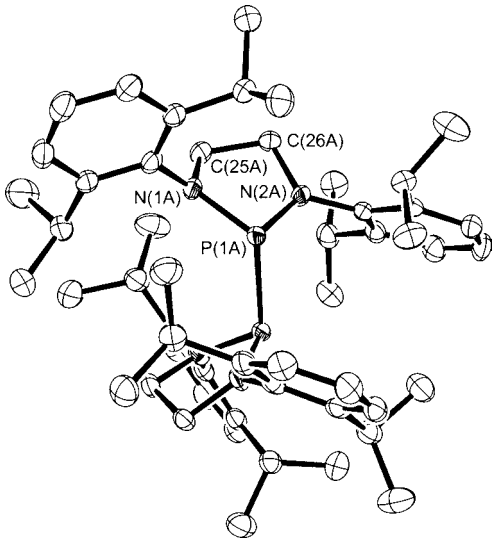

Figure 1. Molecular structure of diphosphine **1**, with thermal ellipsoids projected at the 50% probability level. Hydrogen atoms have been removed for clarity. Selected bond lengths (Å) and angles (deg): P(1A)−N(1A) = 1.7004(17), P(1A)−N(2A) = 1.7269(18), P(1A)−P(1A) = 2.3206(9), N(1A)−C(25A) = 1.474(2), N(2A)−C(26A) = 1.467(2), C(25A)−C(26A) = 1.525(2); N(1A)−P(1A)−N(2A) = 91.74(9), N(1A)−P(1A)−P(1A) = 118.52(6), N(2A)−P(1A)−P(1A) = 96.17(6), C(25A)−N(1A)−P(1A) = 112.33(12), C(26A)−N(2A)−P(1A) = 113.91(13), N(1A)−C(25A)−C(26A) = 106.63(15), N(2A)−C(26A)−C(25A) = 105.00(14).

3.2. EPR Spectroscopy. Dissolution of diphosphine **1** in hexanes to give a pale yellow-orange solution that produced strong EPR signals (Figure 2) indicating that there is phosphinyl present in solution at room temperature. When cooling the sample to 7 °C the EPR signal becomes very weak and has essentially disappeared by −10 °C (Figure S2) but reappears upon reheating to ambient temperatures. This result confirms the reversible dissociation of the P−P bonded dimer (diphosphine) into monomeric radicals at higher temperatures and also agree with the sharpening of the signals in the ^{1}H NMR spectrum that was noted in the synthesis section due to the lack of radical present at lower temperatures.

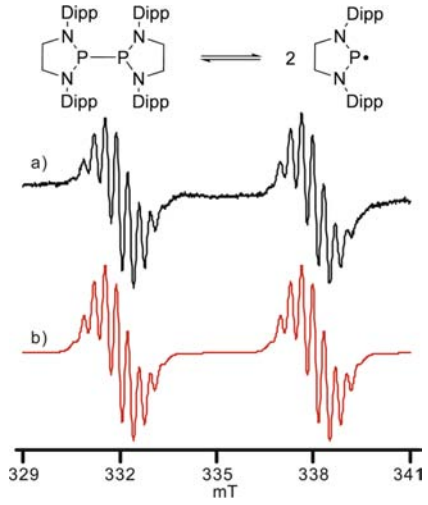

Figure 2. (a) Experimental EPR spectrum of 1.1 mM solution of **1** in hexanes at 22 °C, SW = 120 G, mod. amp = 3 G; and (b) simulated spectrum, a_P = 60.9 G; $a_{N1,2}$ = 3.7 G; a_{H1-4} = 2.9 G; LW = 1.75 G; g = 2.0031.

The phosphinyl radical is kinetically stabilized by the bulky 2,6-diisopropylphenyl groups as well as by delocalization of the unpaired electron over the two nitrogen and four hydrogen atoms in the heterocyclic ring. At 22 °C the spectrum consists of a doublet which is split into nonets (g = 2.0031), consistent with hyperfine coupling to one phosphorus (a_P = 171 MHz), two equivalent nitrogen ($a_{N1,2}$ = 10 MHz), and four equivalent hydrogen (a_{H1-4} = 8.1 MHz) nuclei. The equivalence of the hydrogen nuclei is congruent with dynamic averaging of the four atoms, for which *ab initio* calculations predict hyperfine splittings of 10.9 MHz (2 H) and 2.5 MHz (2 H), with an average value of 6.7 MHz, which is in good agreement with experimental results. In contrast, the recently published EPR

dx.doi.org/10.1021/ic301758k | *Inorg. Chem.* 2012, 51, 11837−11850

spectrum of **L** is a doublet of quintets with no indication of coupling to the hydrogen atoms attached to the heterocyclic core.[31] This can be explained by the nature of the SOMO of **L•**, which in this case has more π-orbital character, such that the hydrogen atoms from the CH backbone are only expected to make a minor contribution to the EPR spectrum. In contrast, the SOMO for phosphinyl **1** shows less planarity in the heterocyclic core, which leads to a larger contribution to the SOMO by the four hydrogen atoms in the carbon backbone (Figure 3). The value of the phosphorus hyperfine coupling

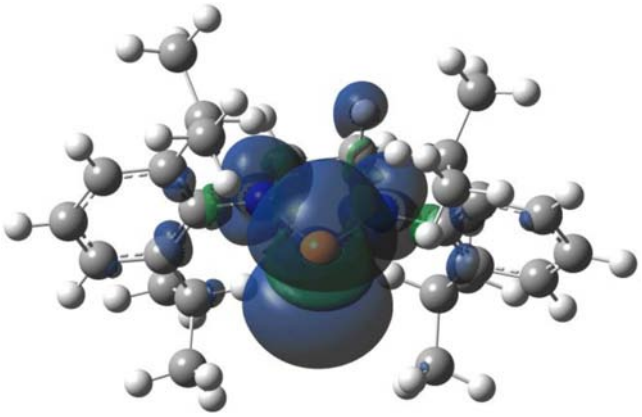

Figure 3. Spin density isosurface for $(H_2C)_2(NDipp)_2P\bullet$ calculated at the B3LYP/6-31G* level in Gaussian 09.[37].

constant suggests that the lone electron is located in a phosphorus orbital of predominantly 3p character, but is slightly smaller than that seen for other similar P(III) radicals.[21] This can be rationalized by the delocalization of the unpaired electron over the nitrogen and hydrogen centers.

Comparison of the EPR parameters of **1** with those of other N-substituted phosphinyls in the literature (Table 2) shows that the hyperfine coupling to ^{31}P is larger than that in the heterocyclic systems **L**, and at the lower end of the hyperfine coupling seen in the acyclic systems. Similarly, the ^{14}N coupling constant in **1** is low compared to the majority of the systems in the literature.

3.3. Electronic Structure Calculations. In order to better understand the electronic and structural implications that the heteroatom substituents have on the diphosphine and phosphinyl stability as well as the consequences of the sterically bulky substituents, we have performed a systematic study based on the following model diphosphines/phosphinyls: $[H_2P]_2$/$H_2P\bullet$, $[(H_2N)_2P]_2$/$(H_2N)_2P\bullet$, $[(H_2C)_2(NH)_2P]_2$/$(H_2C)_2(NH)_2P\bullet$, $[(H_2C)_2(NPh)_2P]_2$/$(H_2C)_2(NPh)_2P\bullet$, and $[(H_2C)_2(NDipp)_2P]_2$/$(H_2C)_2(NDipp)_2P\bullet$. The energetic preferences for these systems have been modeled at various levels of theory and are included in Table 3. Note that all discussion of energies will be based on the B3LYP/6-31+G* level of theory, unless otherwise specified. The most stable optimized structures are shown in Figure 4. See the Supporting Information for complete discussion of the computational approach.

For $[H_2P]_2$ a number of higher symmetry structures were attempted (D_{2h}, D_{2d} and D_2), however we only found three stationary points; the structure with C_2 symmetry gave the most stable structure followed by C_{2h} (0.5 kJ/mol) and C_{2v} (17.4 kJ/mol). The structure is in close agreement with both experimental values and recently calculated values for diphosphane (Table 3). The diphosphine is energetically favored over two equivalents of the phosphinyl monomer, $H_2P\bullet$, by 225.0 kJ/mol, indicating that this is the P−P bond dissociation energy since there is little strain on the P−P bond from the hydrogen substituents. This is significantly higher in energy than that calculated for Me_2P-$PMe_2 \rightarrow 2\ Me_2P\bullet$ (102.6 kJ/mol).[8,9] It should be noted that the barrier to the simultaneous inversion of both phosphorus centers is calculated to be 206.4 kJ/mol ($C_2 \rightarrow D_{2d}$). As expected, this is lower than twice the reported inversion energy for one phosphorus center in diphosphine at a similar level of theory (B3LYP/6-31G(d) 116.4 kJ/mol).[44] Finally, the H−P−H angle has slightly increased from 91.74° in the phosphinyl, $H_2P\bullet$, to 93.83° in the diphosphine.

The $(H_2N)_2P\bullet$ radical optimized with C_2 symmetry as the only stable conformation. In the diphosphine form, there are two stable arrangements both having C_2 symmetry. C_2#1 is 8.0 kJ/mol more stable than the C_2#2 form and the P−P bond

Table 2. EPR Parameters for Various N-Substituted Phosphinyls

cmpd	g	$a(^{31}P)$ MHz (Gauss)[a]	$a(^{14}N)$ MHz (Gauss)[a]	ref
$(H_2C)_2(NDipp)_2P\bullet$	2.0031	171 (60.9)	10 (3.7)	*b*
D	2.007	3×10^1 (9)	1×10^1 (4)	25
G	2.005	2.2×10^2 (78)	*c*	15
L ^{t}Bu	2.00088	1.1×10^2 (41)	16 (5.8)	31
L Mes	2.01775	1.1×10^2 (40)	15 (5.2)	31
L Dipp	2.0248	1.2×10^2 (42)	15 (5.4)	31
$[(Me_3Si)_2N]_2P\bullet$	2.008	258 (91.8)	*d*	6
$[(Me_3Si)_2CH](Me_3Si)_2NP\bullet$	2.008	2.61 (93.0)	*d*	7
$[(Me_3Si)_2CH][(^iPr)_2N]P\bullet$	2.005	1.8×10^2 (63)	10 (3.7)	7
$[(Me_3Si)_2N][(^iPr)_2N]P\bullet$	2.007	217 (77.2)	15 (5.2)	7
	2.0046	213 (75.9)	15.3 (5.45)	10,11
$[Me_3Si][(^tBu)_2N]P\bullet$	2.007	285.1 (101.5)	*d*	7
$[(Me_3Si)(^tBu)N](^iPr)_2NP\bullet$	2.007	208 (74.0)	14 (5.1)	7
$[(Me_3Si)_2CH][(Me_2)N]P\bullet$	2.008	1.8×10^2 (65)	*d*	7
$[(Me_3Si)_2N][Mes]P\bullet$	2.008	272 (96.7)	*d*	7
$[(^iPr)_2N][2,6\text{-}CF_3Ph)P\bullet$	2.006	2.4×10^2 (87)	15 (5.5)	12

[a]The Hyperfine coupling constants are given in the IUPAC recommended units of MHz. The other common unit of Gauss is given in parentheses. [b]This work. [c]No coupling to ^{14}N was observed. [d]Hyperfine coupling constants were not reported.

Table 3. Energenic Preference (E_{diss}) between the Phosphinyl and Diphosphine Systems at Various Levels of Theory[a]

	HF				B3LYP	
method	STO-3G	3-21G	6-31G	6-31+G*	6-31G*	6-31+G*
$[H_2P]_2$	−213.3	−98.4	−138.6	−137.6	−227.5	−225.0
$[(H_2N)_2P]_2$	−156.9	−95.4	−133.5	−120.7	−190.3	−175.8
$[(H_2C)_2(NH)_2P]_2$	−144.1	−32.0	−91.6	−88.3	−147.0	−141.1
$[(H_2C)_2(NPh)_2P]_2$	*b*	−25.3	−56.4	−49.1	−108.2	−100.7
$[(H_2C)_2(NDipp)_2P]_2$	52.7	92.1	113.7	124.4	−8.7	11.6

[a] $E_{diss} = E_{diphosphine} - 2E_{phosphinyl}$. [b] No stable diphosphine form could be found.

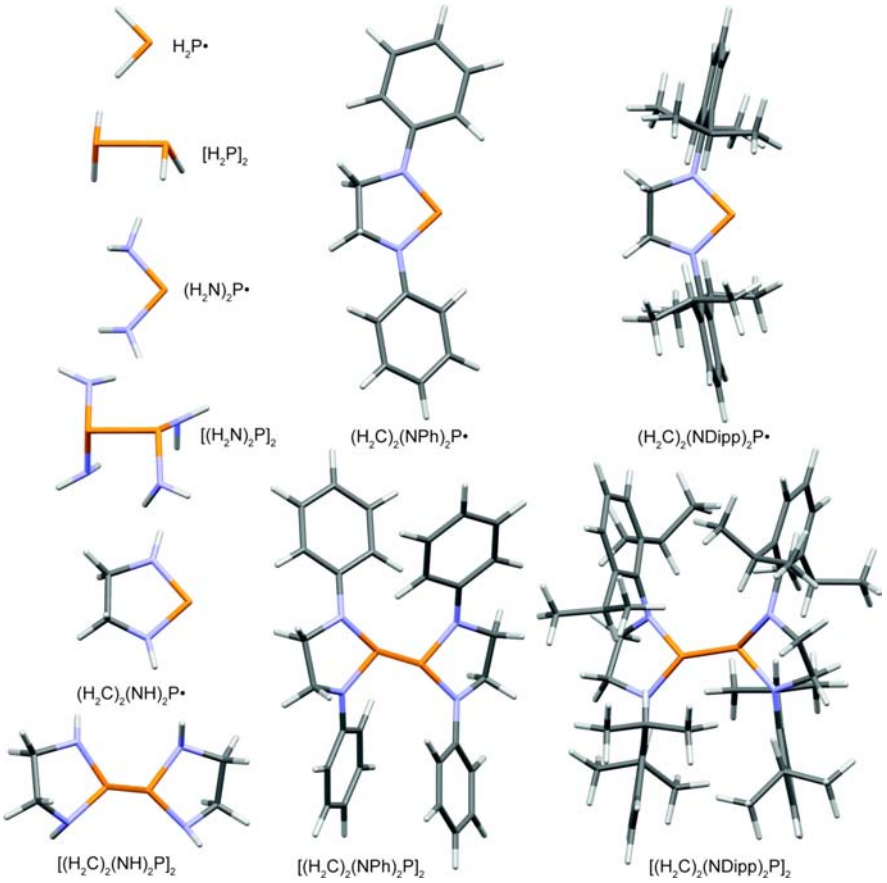

Figure 4. Structures of $H_2P\bullet$, $[H_2P]_2$, $(H_2N)_2P\bullet$, $[(H_2N)_2P]_2$, $(H_2C)_2(NH)_2P\bullet$, $[(H_2C)_2(NH)_2P]_2$, $(H_2C)_2(NPh)_2P\bullet$, $[(H_2C)_2(NPh)_2P]_2$, $(H_2C)_2(NDipp)_2P\bullet$, and $[(H_2C)_2(NDipp)_2P]_2$ optimized at the B3LYP/6-31+G* level of theory.

dissociation energy is calculated to be 175.8 kJ/mol. This is approximately 50 kJ/mol lower than that of the parent diphosphine and can be attributed to the reduced radical character at the phosphorus atom. The calculated Mulliken spin density on phosphorus decreases from 1.069 in $H_2P\bullet$ to 0.914 in $(H_2N)_2P\bullet$. The P−P bond length is identical to that of the parent diphosphine at 2.251 Å. However, the sum of angles at phosphorus in $[(H_2N)_2P]_2$ has increased to 301.04° from 289.30° in the phosphinyl, and the N−P−N angle has increased significantly from 94.92° in the phosphinyl $(H_2N)_2P\bullet$ to 108.44° in $[(H_2N)_2P]_2$.

Moving to the parent heterocycle, $[(H_2C)_2(NH)_2P]_2$/$(H_2C)_2(NH)_2P\bullet$, where the two nitrogen atoms are connected by an ethane spacer to form a five-membered ring, results in some changes to the system including a reduction in the N−P−N bond angle. Two minima were found for the $(H_2C)_2(NH)_2P\bullet$ radical; the structure with C_2 symmetry was found to be slightly more stable than the structure with C_1 symmetry (+6.4 kJ/mol). The C_2 phosphinyl N−P−N angle of 89.81° reflects the constraint of the five-membered heterocycle compared to the noncyclic, diamino version, $(H_2N)_2P\bullet$. The nitrogen atoms in the phosphinyl are pyramidal (Σ of N_{ang} = 343.66°). Moving on to the diphosphine, $[(H_2C)_2(NH)_2P]_2$, the phosphinyl radicals can combine in a number of ways and to simplify this, only the coupling of equivalent rings was considered. Of the "C_2"-type of couplings, the two C_2 monomers can couple (C_2#1, the N−H bonds in a syn−anti = "sa" relationship to the P−P bond), or two different couplings of the C_1 monomer (C_1#2, "ss" and C_1#3, "aa"). All of these are stable. Of the "C_{2h}" couplings, only "aa" #1 and "ss" #2 are possible, and neither is an energy minimum, usually containing both imaginary frequencies of A_u and B_g character. These lead to additional C_2 ("aa", C_2#4; "sa", C_2#5) and C_i structures ("aa", C_i#1; "sa", C_i#2). The "ss" structures are much higher in energy than "aa" structures and often revert to "sa" structures. Overall, the most stable is the C_2#4 structure,

dx.doi.org/10.1021/ic301758k | Inorg. Chem. 2012, 51, 11837−11850

although C_i#1 is nearly isoenergetic (+1.0 kJ/mol). Both are derived from the "C_{2h}", so it appears as though steric clashing between the two ethylene units is enough to disfavor the "C_2" coupling which was favored in the noncyclic system. The diphosphine, $[(H_2C)_2(NH)_2P]_2$, is favored over two phosphinyl units by 141.1 kJ/mol which is approximately 40 kJ/mol lower in energy than in the noncyclic system $[(H_2N)_2P]_2$. The P−P bond length $[(H_2C)_2(NH)_2P]_2$ is similar to the noncyclic version at 2.264 Å. With respect to the phosphinyl monomer, the nitrogen atoms in $[(H_2C)_2(NH)_2P]_2$ have become slightly more pyramidalized (Σ of N_{ang} = 333.86° and 338.21).

Adding phenyl substituents to the heterocyclic phosphinyl system, $(H_2C)_2(NPh)_2P\bullet$, gives rise to a stable C_2 geometry with little change to the NPN angle (90.28°) relative to the parent heterocyclic phosphinyl, $H_2P\bullet$. The phenyl rings are only slightly twisted (19.02°) with respect to the mean plane defined by the heterocycle and the nitrogen atoms are nearly planar (Σ of N_{ang} = 358°). Analysis of the diphosphine, $[(H_2C)_2(NPh)_2P]_2$, reveals two stable C_2 forms that vary by 7.5 kJ/mol. The more stable of the two diphosphines is now only 100 kJ/mol more stable than two phosphinyl units. This is similar to that calculated for $Me_2P{-}PMe_2 \rightarrow 2\ Me_2P\bullet$ (102.6 kJ/mol, UB3LYP/DZP).[9] This is also approximately 40 kJ/mol less stable with respect to the parent heterocycle. The P−P bond length in $[(H_2C)_2(NPh)_2P]_2$ is 2.345 Å, which is over 0.8 Å longer than the parent heterocycle diphosphine, $[(H_2C)_2(NH)_2P]_2$, and is similar to the P−P distance from the crystal structure of **1**. There is little change in the planarity of the nitrogen atoms of $[(H_2C)_2(NPh)_2P]_2$ in comparison with the phosphinyl (Σ of N_{ang} = 356° and 359°).

Finally, moving to the calculations on the full system, $[(H_2C)_2(NDipp)_2P]_2$, we find that it optimizes with C_2 symmetry and the gross structural features are similar to the structure seen in the solid state. There are significant structural distortions that arise from the need of the Dipp groups to accommodate the formation of the P−P bond. The P−P bond is 2.410 Å, significantly longer than in the phenyl-substituted system, but is overestimated by nearly 0.1 Å when compared to that in the solid-state structure of **1**. Again, the nitrogen atoms are nearly planar (Σ of N_{ang} = 357° (both)). The least distorted Dipp ring is twisted from the mean plane of the heterocycle by 53.79°, and the *ipso* carbon is 0.056 Å out of the mean heterocyclic plane. The other Dipp substituent is less twisted from the mean plane of the heterocycle at 82.44° but is significantly bent from the mean heterocyclic plane by 1.040 Å. Overall, these distortions are fewer than when compared to the crystal structure, but this can be attributed to the longer P−P bond in the calculated structure allowing for less overall distortion in the calculated molecule. When comparing the calculated structure of the phosphinyl radical of the full system, it is clear how significant the distortions in the diphosphine are (Figure 5). Taking half of the optimized diphosphine structure and comparing the energy of this "distorted" phosphinyl to that of the optimized phosphinyl structure can be used to calculate the so-called relaxation energy of the system. This has been calculated to vary from 98 to 158 kJ/mol depending on the level of theory used (Table 4).

The relaxation energy of the system can be calculated by taking half of the optimized diphosphine structure and comparing the energy of the "distorted" phosphinyl to that of the optimized phosphinyl structure. This has been investigated by Rankin et al. for $[((Me_3Si)_2CH)_2P]_2$ and related systems.[8,9,29,30,45] We followed a systematic approach and started with the parent diphosphine $[H_2P]_2$ and worked our way up through the more complicated systems. Two scans for each system were performed: one with the coordinates of all atoms fixed and the other with only the P−P bond distance fixed and the other atoms allowed to optimize (relax). All scans were completed at the B3LYP/6-31+G* level of theory except for $[(H_2C)_2(NPh)_2P]_2$ (HF/6-31G*) and $[(H_2C)_2(NDipp)_2P]_2$ (HF/STO-3G) which were limited by the computational time requirements. Nevertheless, these lower-level calculations still provide a reliable picture of the overall energy.

When looking at the scan of the $[H_2P]_2$ (Figure 6A), we see that there is little energy difference between the fixed and relaxed scans, as would be expected since there are few to no steric interactions between the hydrogen substituents. It should be noted that the C_2 structure morphs into a C_{2h} structure

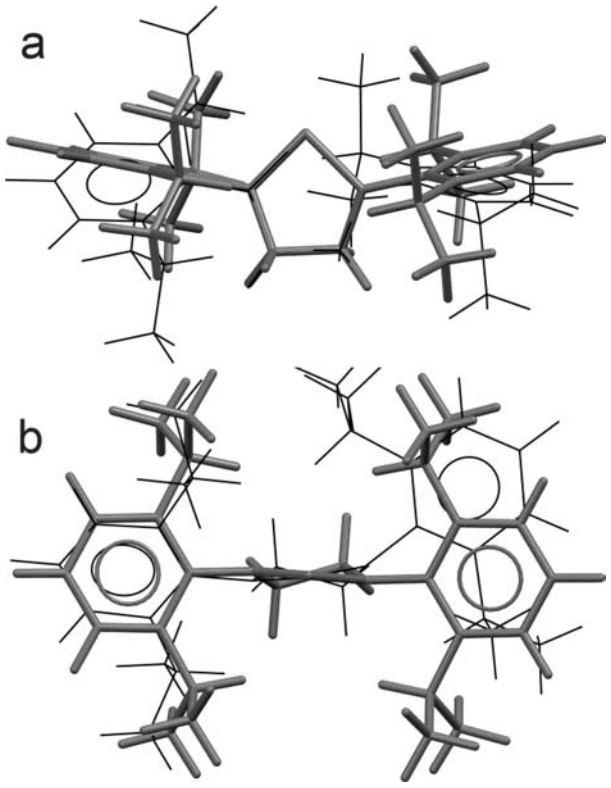

Figure 5. Top (a) and front (b) views of the optimized structure (B3LYP/6-31+G*) of the phosphinyl (gray tubes) overlaid with one-half of the optimized diphosphine structure (black sticks) showing the extreme distortion of the Dipp groups.

Table 4. Relaxation Energies of $[(H_2C)_2(NDipp)_2P]_2$ at Various Levels of Theory[a]

method	E_{relax} (kJ/mol)[b]
HF/STO-3G	135.2
HF/3-21G	105.8
HF/6-31G*	155.4
HF/6-31+G*	158.2
B3LYP/6-31G*	98.0
B3LYP/6-31+G*	104.6

[a]Geometries were optimized using the specified methods. [b]$E_{relax} = 2(E_{phosphinyl} - E_{strained})$, where $E_{strained}$ is the energy from a single-point calculation based on one-half of the optimized structure of the diphosphine.

dx.doi.org/10.1021/ic301758k | *Inorg. Chem.* 2012, 51, 11837−11850

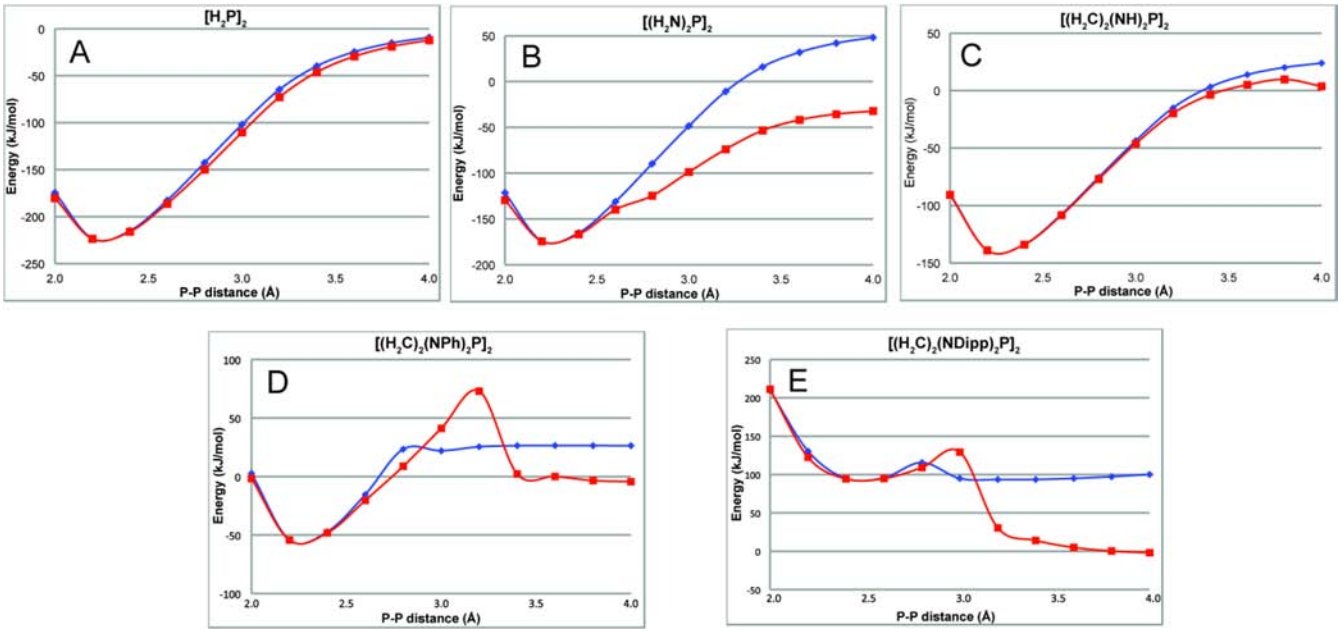

Figure 6. Potential energy scans of diphosphines with P−P bond distances set from 2.0 to 4.0 Å. All structures calculated at the B3LYP/6-31+G* level of theory with the exception of $[(H_2C)_2(NPh)_2P]_2$ (HF/6-31G) and $[(H_2C)_2(NDipp)_2P]_2$ (HF/3-21G). Scans where the atom positions are all frozen are in blue (diamonds). Geometries are taken from the fully optimized structure, and only the P−P distance is varied. Scans where only the P−P bond is fixed and the rest of the molecule is allowed to optimize are shown in red (squares).

between 2.6 and 2.8 Å. At the 4.0 Å distance, there is only 2.9 kJ/mol difference between the fixed and relaxed structures. We see that the energy difference between the structure at the equilibrium bond distance of 2.251 Å and the distance at 4.0 Å (−212.9 kJ/mol) is nearly the same as that calculated for the difference between $[H_2P]_2$ and two $H_2P\bullet$ monomers (−225.0 kJ/mol).

Moving onto the scan of $[(H_2N)_2P]_2$ (Figure 6B), we see that the fixed C_2 structure at 4 Å is significantly higher in energy (48.3 kJ/mol) relative to that of two phosphinyl radicals. At between 3.2 and 3.4 Å the energy of the diphosphine passes though the equivalence point with the energy of two phosphinyls. However, in the relaxed scans, we see that the system never becomes equivalent (or even close!) in energy to two phosphinyls, and at 4 Å it is still 32.3 kJ/mol more stable. This can be attributed to a rotation that occurs about the P−P bond which allows for hydrogen bonds to form between the amine hydrogen atoms on one heterocycle and the lone pair on an amine on the other heterocycle. Due to this hydrogen-bonding interaction, it is not feasible to make a comparison of the relaxation energy involved in this system.

In the parent heterocyclic system, $[(H_2C)_2(NH)_2P]_2$, we see that the fixed and relaxed systems have similar energies with P−P bond distances from 2 to 2.8 Å (Figure 6C). At 3 Å the two diverge with the fixed system increasing in energy at a greater rate than the relaxed system. At about 3.8 Å (+9.8 kJ/mol) the relaxed system levels off and begins to drop in energy and approach 0 kJ/mol at the 4 Å distance as would be expected. The combined relaxation and P−P bond energy of the system at 4 Å distance is 20.1 kJ/mol.

When phenyl substituents are added to the heterocycle to give $[(H_2C)_2(NPh)_2P]_2$, the fixed system increases in energy from the low-energy diphosphine at approximately 2.2 Å (−56.4 kJ/mol) and increases in energy until about 2.8 Å, where it levels off at around +26 kJ/mol relative to two phosphinyl radicals (Figure 6D). This equates to a relaxation energy for the diphenyl system to be approximately 52 kJ/mol. Looking at the relaxed scans we see that the system increases in energy from 2.2 Å to about 3.2 Å (+73.0 kJ/mol) and then decreases in energy and levels off between 3.4 Å (2.17 kJ/mol) and 4.0 Å (−4.4 kJ/mol). The extremely high energy at 3.2 Å can be attributed to the strong interactions of the phenyl substituents as the P−P bond moved from a nearly eclipsed configuration to a staggered configuration.

Finally, looking at the full system, $[(H_2C)_2(NDipp)_2P]_2$, both the fixed and relaxed scans come to a minimum between 2.4 Å and 2.6 Å (approximately +95 kJ/mol, Figure 6E). For the fixed scan the energy increases slightly at 2.8 Å (+115.6 kJ/mol) then drops and levels off to +100.1 kJ/mol at 4 Å. For the relaxed scan we note a slight increase in energy at 3 Å (+129.3 kJ/mol) and then a significant drop in energy as the P−P distance increases. At 4 Å this energy is essentially 0 kJ/mol relative to the energy of the calculated phosphinyl $(H_2C)_2(NDipp)_2P\bullet$. This can be attributed to the relaxation energy of the ligand and the P−P bond energy in the system.

3.4. Reactivity with Chalcogens and P_4. A dry, degassed toluene solution of diphosphine **1** was reacted with approximately one atmosphere of gaseous O_2 at room temperature. Over a period of 30 min the yellow-orange color of the diphosphine solution had completely disappeared, leaving a colorless solution. Analysis by ^{31}P NMR spectroscopy revealed quantitative conversion to a single product: a singlet with a chemical shift of δ 3.4 ppm indicating the possible formation of a P(V) product. The product **3** crystallizes as large colorless blocks from an evaporating toluene solution (Scheme 2.

Analysis of the product by single-crystal X-ray crystallography revealed, surprisingly, the phosphinic acid anhydride **3** (Figure 7) in the monoclinic space group $P2(1)/c$. Crude analysis of the connectivity shows insertion of an oxygen atom between the phosphorus atoms as well as oxidation of both phosphorus atoms to P(V) with two additional oxygen atoms.

dx.doi.org/10.1021/ic301758k | *Inorg. Chem.* 2012, 51, 11837−11850

Scheme 2. Reaction Products of Chalcogens and P_4 with 1

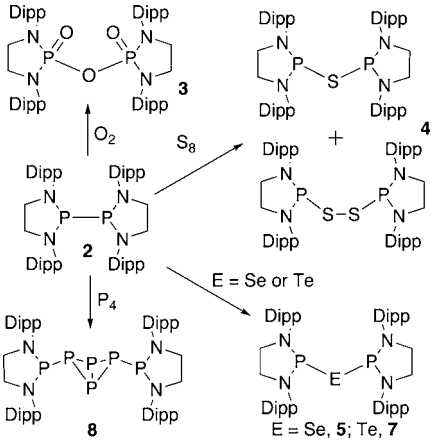

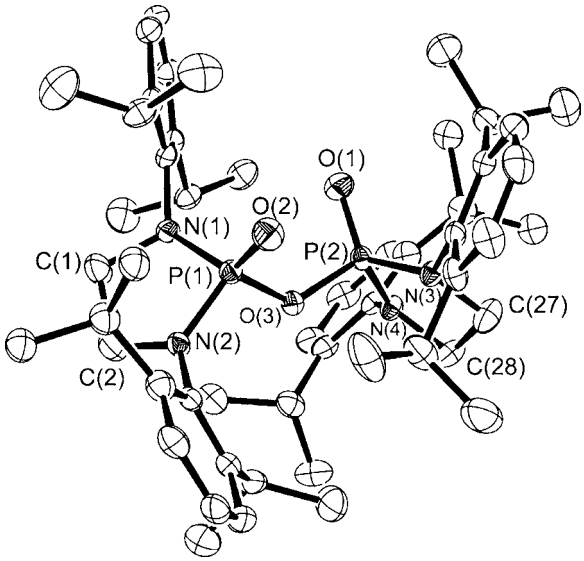

Figure 7. Molecular structure of phosphinic acid anhydride **3**, with thermal ellipsoids projected at the 50% probability level. Hydrogen atoms have been removed for clarity. Selected bond lengths (Å) and angles (deg): P(1)−O(2) = 1.444(2), P(1)−O(3) = 1.6290(18), P(1)−N(2) = 1.647(2), P(1)−N(1) = 1.660(2), C(1)−N(1) = 1.464(3), C(1)−C(2) = 1.507(4), O(1)−P(2) = 1.446(2), P(2)−O(3) = 1.6270(18), P(2)−N(3) = 1.641(2), P(2)−N(4) = 1.661(2), C(2)−N(2) = 1.462(3), N(3)−C(27) = 1.467(3), N(4)−C(28) = 1.470(3), C(27)−C(28) = 1.506(4); O(2)−P(1)−O(3) = 108.25(11), O(2)−P(1)−N(2) = 118.31(12), O(3)−P(1)−N(2) = 104.46(10), O(2)−P(1)−N(1) = 122.09(12), O(3)−P(1)−N(1) = 107.66(10), N(2)−P(1)−N(1) = 94.20(11), N(1)−C(1)−C(2) = 107.1(2), C(1)−N(1)−P(1) = 112.52(17), O(1)−P(2)−O(3) = 108.93(11), O(1)−P(2)−N(3) = 118.42(11), O(3)−P(2)−N(3) = 103.91(10), O(1)−P(2)−N(4) = 121.37(11), O(3)−P(2)−N(4) = 107.99(10), N(3)−P(2)−N(4) = 94.27(11), N(2)−C(2)−C(1) = 105.6(2), C(2)−N(2)−P(1) = 113.49(17), C(27)−N(3)−P(2) = 112.99(17), P(2)−O(3)−P(1) = 125.08(11), C(28)−N(4)−P(2) = 112.43(17), N(3)−C(27)−C(28) = 105.4(2), N(4)−C(28)−C(27) = 106.4(2).

Upon initial analysis of the structure it appears that the significant twisting of the O═P−O−P═O fragment is necessary to help alleviate steric strain in the system. However, it is clear that, when comparing the structure with other phosphinic acid anhydrides, this strong twisting is not a result of sterics but is typical of this framework.[46,47] For example, in the dimethylphosphinic acid anhydride, $Me_2P(O)-O-P(O)-Me_2$[46] **A**, the O−P−P−O dihedral is 84.91° (no s.u. given), whereas in **3** the O1−P2−P1−O2 dihedral is 82.5(2)°. The P═O distances in compound **3** (1.444(2) Å and 1.446(2) Å) are slightly shorter than that in **A** (1.471(2) Å) and the P−O distances (1.627(2) Å and 1.629(2) Å) are statistically the same as in compound **A** (1.6256(9) Å). Finally, the P−O−P angle (125.08(11)°) in compound **3** is similar to that in compound **A** at 124.6(1)°. There does not appear to be any significant distortions to either heterocycle or the four Dipp groups surrounding the diphosphoester core, and there are no significant long distance interactions within the crystal lattice. Perusal of the literature shows that the formation of phosphinic acid anhydrides can occur through a number of routes including the following: reaction of a diphosphine with hydrogen peroxide solutions,[47] thermal dehydration of phosphinic acids,[48] reaction of phosphinic acid alkyl esters with *gem*-dihalides,[49] and the reaction of disubstituted phosphoric chlorides with sodium phenylphosphinate.[50]

Reaction of diphosphine **1** with excess elemental sulfur in toluene results in the formation of a colorless solution with two signals in the ^{31}P NMR spectrum in approximately a 1 (δ = 154 ppm): 9 (δ = 136 ppm) ratio. Colorless crystals of compound **4** were grown from a slowly evaporating toluene solution to give large colorless blocks. In order to ascertain the composition of the product, analysis by X-ray crystallography was performed. Interestingly, we found that the two halves of the diphosphine are present in the solid state, and through careful analysis of the disorder present we found that the sulfide and disulfide cocrystallize in an 87:13 ratio roughly matching the ratio of products seen in the ^{31}P NMR spectrum (Figure 8). This product is similar to that recently reported by Cowley et al. in the reaction of $(Me_3Si)_2CH)_2P-P(CH(SiMe_3)_2)_2$ with ele-

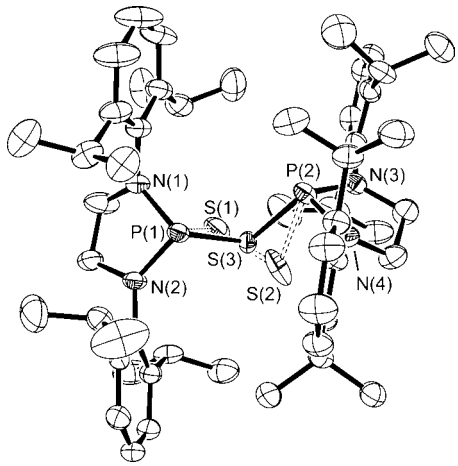

Figure 8. Molecular structure of sulfide (87%): disulfide (13%) **4**, with thermal ellipsoids projected at the 50% probability level. Hydrogen atoms have been removed for clarity. Selected bond lengths (Å) and angles (deg): S(2)−S(1) = 1.952(16), P(1)−N(1) = 1.682(2), P(1)−N(2) = 1.689(2), P(1)−S(3) = 2.1905(15), P(1)−S(1) = 2.237(4), P(2)−N(4) = 1.691(3), P(2)−N(3) = 1.695(2), P(2)−S(3) = 2.1912(14), P(2)−S(2) = 2.249(5); P(1)−S(3)−P(2) = 95.25(4), N(1)−P(1)−N(2) = 89.82(12), N(1)−P(1)−S(3) = 108.58(8), N(2)−P(1)−S(3) = 102.96(9), N(1)−P(1)−S(1) = 83.8(3), N(2)−P(1)−S(1) = 90.06(19), N(4)−P(2)−N(3) = 89.90(11), N(4)−P(2)−S(3) = 108.50(9), N(3)−P(2)−S(3) = 102.79(9), N(4)−P(2)−S(2) = 85.9(3), N(3)−P(2)−S(2) = 90.8(2), S(1)−S(2)−P(2) = 90.7(4), S(2)−S(1)−P(1) = 88.2(3).

dx.doi.org/10.1021/ic301758k | *Inorg. Chem.* 2012, 51, 11837−11850

mental sulfur.[51] However, in that case, the authors report that all of their reaction attempts resulted in intractable mixtures, and in one case were only able to isolate one single crystal for analysis. This implies that the reactivity of our system may be slightly more controlled, allowing for the isolation of specific species. Analysis of the major sulfide component of the structure reveals an internal P---P distance of 3.237(3) Å with a P−S−P angle of 93.25(4)° and P−S distances of 2.1905(15) Å (P1−S3) and 2.1912(14) Å (P2−S3). The P−S distances in $(Me_3Si)_2CH)_2P-S-P(CH(SiMe_3)_2)_2$ are slightly shorter (2.182(2) Å, 2.141(2) Å) and the P−S−P angle is slightly larger (98.36(6)°) than in **4**. The minor disulfide component, has P−S distances of 2.237(4) Å and 2.245(5) Å with an S−S distance of 1.952(16) Å. Although the P−S bonds are slightly elongated relative to similar bonds in the major sulfide component, they are in line with the P−S bond lengths (2.1930(10) Å) in $Ph_2(S)P-S-S-P(S)Ph_2$.[52] The S−S bond (1.925(16) Å) is shorter by approximately 0.1 Å than in *P*−PhS−SPh (2.022(2) Å) or *M*−PhS−SPh (2.0289(7) Å),[53] but our value may not be completely reliable since it is a minor component (13%) in the structure. Analysis of the packing in the structure shows no significant long distance interactions.

Reaction of compound **1** with elemental selenium and tellurium results in the insertion of the chalcogen between the two phosphorus atoms to form diphosphoselenide **5** and diphosphotelluride **7**. In their solid-state analysis, both structures proved to be visually similar, and so the graphic for the structure of **5** has been placed in the Supporting Information. In the case of selenium, the stoichiometry of the reaction proved to be important. Stirring equimolar amounts of selenium and **1** overnight gave the diphosphoselenide **5** as colorless crystals upon workup in good yield. The ^{31}P NMR spectrum reveals a signal at 160 ppm with satellites resulting from coupling to Se (^{77}Se: spin $^1/_2$, 7.6% abundant; $^1J_{P-Se}$ = 141 Hz). Addition of excess selenium resulted in a number of products by ^{31}P NMR, and we were able to isolate a single crystal of a mixed P(III) and P(V) system **6** (see Supporting Information) where a selenium atom inserted in the P−P bond and a second selenium atom oxidized one of the phosphorus centers. No further attempts to isolate **6** were attempted, as subsequent reactions could not be controlled.

Crystals of **5** were grown by slow evaporation of a toluene solution. The solid-state structure reveals four molecules in the asymmetric unit. The P−Se distances range from 2.3440(18) Å and 2.3712(19) Å. This is in line with the report of Cowley et al. where reaction of **J** with elemental selenium gave the diphosphoselenide, where the P−Se distances are 2.295(2) and 2.3333(2) Å. The P−Se−P angles range from 85.44(7)° to 86.40(6)°. This is slightly more acute than the analogous angle in sulfur derivative **4** and also Cowley's diphosphoselenide (96.65(6)°).

Reaction of **1** with an excess of elemental tellurium resulted in the formation of **7** as the only product by ^{31}P spectroscopy. Upon workup, **7** was isolated as colorless crystals from toluene. The crystal structure (Figure 9) reveals two molecules in the asymmetric unit. The P−Te distances range from 2.582(7) Å and 2.587(8) Å and are in line with Cowley's diphosphinotelluride.

Finally, we examined the reaction of the diphosphine with white phosphorus. Mixing the orange−red toluene solution of **1** with one equivalent of P_4 at room temperature resulted in the formation of a golden-yellow solution. Analysis by ^{31}P NMR spectroscopy revealed the formation of a new product **8** with

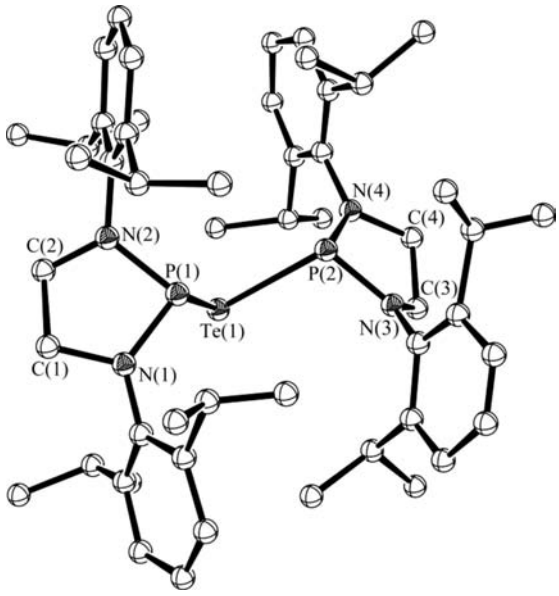

Figure 9. Molecular structure of telluride **7** with thermal ellipsoids projected at the 50% probability level. Hydrogen atoms have been removed for clarity. Selected bond lengths (Å) and angles (deg): Te1−P2 = 2.584(7), Te1−P1 = 2.587(8), P4−N7 = 1.63(2), P4−N8 = 1.71(2), P2−N4 = 1.69(2), P2−N3 = 1.72(2), P1−N1 = 1.69(2), P1−N2 = 1.71(2), P2−Te1−P1 = 83.0(2), N4−P2−N3 = 90.9(12), N4−P2−Te1 = 103.1(8), N3−P2−Te1 = 109.0(9), N1−P1−N2 = 91.1(11), N1−P1−Te1 = 103.1(9), N2−P1−Te1 = 111.2(8).

signals containing a complex splitting pattern located at approximately δ = 160, −110, and −350 ppm. The location of the upfield signals is typical of a P_4 butterfly-type structure.[54] Recently, Lappert et al. reported the reaction of white phosphorus with a diphosphine that is known to undergo homolytic cleavage of the P−P bond at elevated temperatures to give a P_4 butterfly-type structure capped by two P(N-$(SiMe_3)_2)(N^iPr_2)$ fragments.[10] Simulating the spectrum for **8** as an AA′MM′X_2 spin system gave a reliable model (Figure 9).

Crystals of **8** were grown from a toluene solution over several days at −35 °C. Indeed, analysis by single-crystal X-ray diffraction revealed a system of six phosphorus atoms that has a butterfly-type P_4 core capped by the two halves of diphosphine **1**. The system crystallizes in the $P4_12_12$ space group, and the P_4 core lies on a two-fold rotation axis, making the molecule symmetric across the butterfly core (Figure 10). The heterocycles are in a *trans,trans*-geometry with respect to the P_4 core, thus minimizing any steric interactions between the large Dipp groups. The P−P bonds range from 2.2894(12) Å for the $P_{heterocycle}-P_{butterfly}$ bond to a relatively short 2.1571(17) Å for the bridgehead P−P bond. This bond is 0.05 Å shorter than in white phosphorus (2.209 Å[55,56]) and is characteristic of butterfly structures such as these;[10,57−62] calculations by Schoeller et al. show that π-donating heteroatoms attached to the butterfly core cause a shortening of this bond.[63] The angle of the "wings" is 85.03(4)° and is similar to that in $[(Me_3Si)_2N)(^iPr_2N)P]_2P_4$[10] (84.65°(no s.u. given)) and $[(^iPr_2N)_2P]_2P_4$[62] (84.36°(no s.u. given)). Analysis of the heterocyclic portion of the molecules shows that the nitrogen atoms are planar (Σ of N_{ang} = 358.9(8)° and 360.0(6)°) and the phosphorus atom in the heterocycle is pyramidal, as expected (Σ of P_{ang} = 296.4(4)°). It should be noted that there are no significant long distance interactions within the crystal lattice.

dx.doi.org/10.1021/ic301758k | *Inorg. Chem.* 2012, 51, 11837−11850

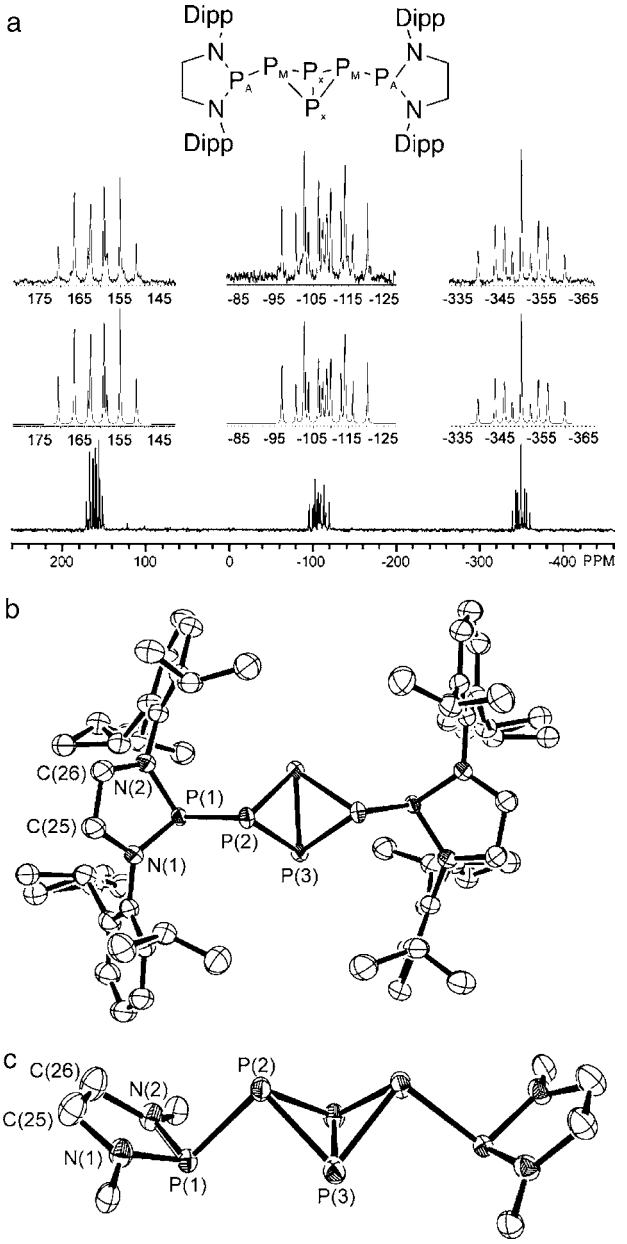

Figure 10. (a) NMR simulation for compound **8**: Experimental data collected at 24.3 MHz. Expansion (above) is experimental coupling used to simulate (lower) coupling for the P_6 core. Modeling of the P_6 system core as AA′MM′X_2 yielded: $^{31}P\{^1H\}$: δ_A = 160.7 ppm, δ_M = −108.2 ppm, δ_X = −349.5 ppm, $J_{AM} = J_{A'M'}$ = −214.9 Hz, $J_{MX} = J_{M'X}$ = −152.8 Hz, $J_{AX} = J_{A'X}$ = +99.2 Hz, $J_{MM'}$ = +101.1 Hz, $J_{AM'} = J_{A'M}$ = −61.2 Hz. (b) Molecular structure of compound **8**, with thermal ellipsoids projected at the 50% probability level. (c) Molecular core of compound **8** in the solid state; note that all but the *ipso*-carbons of the bulky Dipp groups have been removed. All hydrogen atoms have been removed for clarity. Selected bond lengths (Å) and angles (deg): P(1)−N(1) = 1.693(3), P(1)−N(2) = 1.693(3), P(1)−P(2) = 2.2894(12), P(2)−P(3) = 2.2182(12), P(2)−P(3′) = 2.2277(12), P(3)−P(3′) = 2.1571(17), P(3)−P(2) = 2.2183(12), N(1)−C(25) = 1.430(5), N(2)−C(26) = 1.457(5), C(25)−C(26) = 1.470(5), N(1)−P(1)−N(2) = 90.60(14), N(1)−P(1)−P(2) = 102.79(11), N(2)−P(1)−P(2) = 103.04(11), P(3)−P(2)−P(3) = 58.05(4), P(3)−P(2)−P(1) = 92.89(5), P(3)−P(2)−P(1) = 92.84(4), P(3)−P(3′)−P(2) = 61.20(4), P(3′)−P(3)−P(2) = 60.75(4), P(2)−P(3)−P(2) = 80.27(5), C(26)−N(2)−P(1) =115.1(2), N(1)−C(25)−C(26) = 110.0(3), N(2)−C(26)−C(25) = 107.7(3).

CONCLUSIONS

(1) We have prepared a new diphosphine **1** that is based on a heterocyclic 1,3,2-diazaphospholidine framework. The diphosphine is prepared in multigram quantities from the phosphorus chloride. The reaction is clean (quantitative by ^{31}P NMR spectroscopy); however, the isolated yields are moderate (74%) due to the extreme solubility of the system in common hydrocarbons.

(2) The diphosphine **1** exists as a dimer in the solid state. Solution EPR spectroscopy shows that there is phosphinyl present in solutions at room temperature and the phosphinyl−diphosphine equilibrium is completely shifted to diphosphine at −10 °C. EPR data show that the unpaired electron density primarily resides on the phosphorus atom but is also delocalized over the nitrogen atoms as well as the hydrogen atoms in the ligand backbone.

(3) The diphosphine reacts with elemental oxygen, sulfur, selenium, tellurium, and white phosphorus at ambient temperatures to give phosphinic acid anhydride **3**, sulfide/disulfide **4**, selenide **5**, telluride **7**, and phosphorus cluster **8**, respectively.

(4) Electronic structure calculations show that, as you move from the parent diphosphine $[H_2P]_2$ to amino-substituted $[(H_2N)_2P]_2$, cyclic amino $[(H_2C)_2(NH)_2P]_2$ and then add bulky substituents to the amino group (Ph or Dipp), the phosphinyl becomes favored over the diphosphine. Potential energy scans of the systems, while varying the P−P bond distance, give a clear picture of the effects that the ligands have on the breakage of the P−P bond. In the full system $[(H_2C)_2(NDipp)_2P]_2$, there is a significant amount of relaxation energy stored in the ligands (52.3 kJ/mol; B3LYP/6-31+G*) that is manifested in distortion of the Dipp groups.

ASSOCIATED CONTENT

Supporting Information

Crystallographic information files (CIF), detailed computational results (including XYZ files), the variable-temperature ^1H NMR spectrum of **1**, and ORTEP diagrams of **1** and **6**. This material is available free of charge via the Internet at http://pubs.acs.org.

AUTHOR INFORMATION

Corresponding Author

jason.masuda@smu.ca.

Notes

The authors declare no competing financial interest.

ACKNOWLEDGMENTS

We acknowledge the Natural Sciences and Engineering Research Council of Canada (NSERC) for financial support of this work (Alexander Graham Bell Canada Graduate Scholarship to N.A.G. and Discovery Grants to J.D.M. and C.C.P.). The Canadian Foundation for Innovation Leaders Opportunity Fund, the Nova Scotia Research and Innovation Trust, and the NSERC Research Tools and Instruments Grants Program are thanked for providing funding for equipment. We thank the Atlantic Computational Excellence Network (ACEnet) for access to computational facilities and Dr. Kathy Robinson and Dr. Charles Campana for pointers on dealing with crystallographic disorder. Prof. René Boeré (University of Lethbridge) is thanked for assistance with interpreting EPR spectra. The reviewers are thanked for providing insightful comments, which we hope were fully addressed.

REFERENCES

(1) Gomberg, M. *J. Am. Chem. Soc.* **1900**, *22*, 757−771.
(2) Hicks, R. G., Ed. *Stable Radicals: Fundamentals and Applied Aspects of Odd-Electron Compounds*; John Wiley & Sons: New York, 2010.
(3) Walling, C.; Pearson, M. S. *Top. Phosphorus Chem.* **1966**, *3*, 1−56.
(4) Schmidt, U.; Kabitzke, K.; Markau, K.; Mueller, A. *Chem. Ber.* **1966**, *99*, 1497−1501.
(5) Kochi, J. K.; Krusic, P. J. *J. Am. Chem. Soc.* **1969**, *91*, 3944−3946.
(6) Gynane, M. J. S.; Hudson, A.; Lappert, M. F.; Power, P. P.; Goldwhite, H. *J. Chem. Soc., Chem. Commun.* **1976**, 623−624.
(7) Gynane, M. J. S.; Hudson, A.; Lappert, M. F.; Power, P. P.; Goldwhite, H. *J. Chem. Soc., Dalton Trans.* **1980**, 2428−2433.
(8) Hinchley, S. L.; Morrison, C. A.; Rankin, D. W. H.; Macdonald, C. L. B.; Wiacek, R. J.; Cowley, A. H.; Lappert, M. F.; Gundersen, G.; Clyburne, J. A. C.; Power, P. P. *Chem. Commun.* **2000**, 2045−2046.
(9) Hinchley, S. L.; Morrison, C. A.; Rankin, D. W.; Macdonald, C. L.; Wiacek, R. J.; Voigt, A.; Cowley, A. H.; Lappert, M. F.; Gundersen, G.; Clyburne, J. A.; Power, P. P. *J. Am. Chem. Soc.* **2001**, *123*, 9045−9053.
(10) Bezombes, J.; Hitchcock, P. B.; Lappert, M. F.; Nycz, J. E. *Dalton Trans.* **2004**, 499−501.
(11) Bezombes, J.; Borisenko, K. B.; Hitchcock, P. B.; Lappert, M. F.; Nycz, J. E.; Rankin, D. W. H.; Robertson, H. E. *Dalton Trans.* **2004**, 1980−1988.
(12) Dumitrescu, A.; Rudzevich, V. L.; Romanenko, V. D.; Mari, A.; Schoeller, W. W.; Bourissou, D.; Bertrand, G. *Inorg. Chem.* **2004**, *43*, 6546−6548.
(13) Agarwal, P.; Piro, N. A.; Meyer, K.; Mueller, P.; Cummins, C. C. *Angew. Chem., Int. Ed.* **2007**, *46*, 3111−3114.
(14) Back, O.; Celik, M. A.; Frenking, G.; Melaimi, M.; Donnadieu, B.; Bertrand, G. *J. Am. Chem. Soc.* **2010**, *132*, 10262−10263.
(15) Back, O.; Donnadieu, B.; von Hopffgarten, M.; Klein, S.; Tonner, R.; Frenking, G.; Bertrand, G. *Chem. Sci.* **2011**, *2*, 858−861.
(16) Ishida, S.; Hirakawa, F.; Iwamoto, T. *J. Am. Chem. Soc.* **2011**, *133*, 12968−12971.
(17) Sheberla, D.; Tumanskii, B.; Tomasik, A. C.; Mitra, A.; Hill, N. J.; West, R.; Apeloig, Y. *Chem. Sci.* **2010**, *1*, 234−241.
(18) Roberts, B. P. *Adv. Free-Radical Chem.* **1980**, *6*, 225−289.
(19) Power, P. P. *Chem. Rev.* **2003**, *103*, 789−809.
(20) Marque, S.; Tordo, P. *Top. Curr. Chem.* **2005**, *250*, 43−76.
(21) Armstrong, A.; Chivers, T.; Boere, R. T. *ACS Symp. Ser.* **2006**, *917*, 66−80.
(22) Ndiaye, B.; Bhat, S.; Jouaiti, A.; Berclaz, T.; Bernardinelli, G.; Geoffroy, M. *J. Phys. Chem. A* **2006**, *110*, 9736−9742.
(23) Ito, S.; Kikuchi, M.; Yoshifuji, M.; Arduengo, A. J., III; Konovalova, T. A.; Kispert, L. D. *Angew. Chem., Int. Ed.* **2006**, *45*, 4341−4345.
(24) Ito, S.; Kikuchi, M.; Sugiyama, H.; Yoshifuji, M. *J. Organomet. Chem.* **2007**, *692*, 2761−2767.
(25) Back, O.; Donnadieu, B.; Parameswaran, P.; Frenking, G.; Bertrand, G. *Nature Chem.* **2010**, *2*, 369−373.
(26) Kinjo, R.; Donnadieu, B.; Bertrand, G. *Angew. Chem., Int. Ed.* **2010**, *49*, 5930−5933.
(27) Cetinkaya, B.; Hudson, A.; Lappert, M. F.; Goldwhite, H. *J. Chem. Soc., Chem. Commun.* **1982**, 609−610.
(28) Borisenko, K. B.; Rankin, D. W. H. *J. Chem. Soc., Dalton Trans.* **2002**, 3135−3141.
(29) Borisenko, K. B.; Rankin, D. W. H. *Inorg. Chem.* **2003**, *42*, 7129−7136.
(30) Borisenko, K. B.; Hinchley, S. L.; Rankin, D. W. H. *ACS Symp. Ser.* **2006**, *917*, 94−107.
(31) Edge, R.; Less, R. J.; McInnes, E. J. L.; Muether, K.; Naseri, V.; Rawson, J. M.; Wright, D. S. *Chem. Commun.* **2009**, 1691−1693.
(32) Foerster, D.; Dilger, H.; Ehret, F.; Nieger, M.; Gudat, D. *Eur. J. Inorg. Chem.* **2012**, *25*, 2989−2994.
(33) Caputo, C. A.; Price, J. T.; Jennings, M. C.; McDonald, R.; Jones, N. D. *Dalton Trans.* **2008**, 3461−3469.
(34) Abrams, M. B.; Scott, B. L.; Baker, R. T. *Organometallics* **2000**, *19*, 4944−4956.
(35) Forgeron, M. A. M.; Gee, M.; Wasylishen, R. E. *J. Phys. Chem. A* **2004**, *108*, 4895−4908.
(36) Frisch, M. J.; Trucks, G. W.; Schlegel, H. B.; Scuseria, G. E.; Robb, M. A.; Cheeseman, J. R.; Montgomery, J. A., Jr.; Vreven, T.; Kudin, K. N.; Burant, J. C.; Millam, J. M.; Iyengar, S. S.; Tomasi, J.; Barone, V.; Mennucci, B.; Cossi, M.; Scalmani, G.; Rega, N.; Petersson, G. A.; Nakatsuji, H.; Hada, M.; Ehara, M.; Toyota, K.; Fukuda, R.; Hasegawa, J.; Ishida, M.; Nakajima, T.; Honda, Y.; Kitao, O.; Nakai, H.; Klene, M.; Li, X.; Knox, J. E.; Hratchian, H. P.; Cross, J. B.; Bakken, V.; Adamo, C.; Jaramillo, J.; Gomperts, R.; Stratmann, R. E.; Yazyev, O.; Austin, A. J.; Cammi, R.; Pomelli, C.; Ochterski, J. W.; Ayala, P. Y.; Morokuma, K.; Voth, G. A.; Salvador, P.; Dannenberg, J. J.; Zakrzewski, V. G.; Dapprich, S.; Daniels, A. D.; Strain, M. C.; Farkas, O.; Malick, D. K.; Rabuck, A. D.; Raghavachari, K.; Foresman, J. B.; Ortiz, J. V.; Cui, Q.; Baboul, A. G.; Clifford, S.; Cioslowski, J.; Stefanov, B. B.; Liu, G.; Liashenko, A.; Piskorz, P.; Komaromi, I.; Martin, R. L.; Fox, D. J.; Keith, T.; Al-Laham, M. A.; Peng, C. Y.; Nanayakkara, A.; Challacombe, M.; Gill, P. M. W.; Johnson, B.; Chen, W.; Wong, M. W.; Gonzalez, C.; and Pople, J. A. *Gaussian03*, Revision D.02; Gaussian, Inc.: Wallingford CT, 2004.
(37) Frisch, M. J.; Trucks, G. W.; Schlegel, H. B.; Scuseria, G. E.; Robb, M. A.; Cheeseman, J. R.; Scalmani, G.; Barone, V.; Mennucci, B.; Petersson, G. A.; Nakatsuji, H.; Caricato, M.; Li, X.; Hratchian, H. P.; Izmaylov, A. F.; Bloino, J.; Zheng, G.; Sonnenberg, J. L.; Hada, M.; Ehara, M.; Toyota, K.; Fukuda, R.; Hasegawa, J.; Ishida, M.; Nakajima, T.; Honda, Y.; Kitao, O.; Nakai, H.; Vreven, T.; Montgomery, J. A., Jr.; Peralta, J. E.; Ogliaro, F.; Bearpark, M.; Heyd, J. J.; Brothers, E.; Kudin, K. N.; Staroverov, V. N.; Kobayashi, R.; Normand, J.; Raghavachari, K.; Rendell, A.; Burant, J. C.; Iyengar, S. S.; Tomasi, J.; Cossi, M.; Rega, N.; Millam, J. M.; Klene, M.; Knox, J. E.; Cross, J. B.; Bakken, V.; Adamo, C.; Jaramillo, J.; Gomperts, R.; Stratmann, R. E.; Yazyev, O.; Austin, A. J.; Cammi, R.; Pomelli, C.; Ochterski, J. W.; Martin, R. L.; Morokuma, K.; Zakrzewski, V. G.; Voth, G. A.; Salvador, P.; Dannenberg, J. J.; Dapprich, S.; Daniels, A. D.; Farkas, Ö.; Foresman, J. B.; Ortiz, J. V.; Cioslowski, J.; Fox, D. J. *Gaussian09*, Revision A.02, Gaussian, Inc.: Wallingford CT, 2009.
(38) Duling, D. R. *J. Magn. Reson., Ser. B* **1994**, *104*, 105−110.
(39) *APEX II, SAINT+ and SADABS*; Bruker AXS Inc.: Madison, WI, 2008.
(40) Sheldrick, G. M. *Acta Crystallogr., Sect. A* **2008**, *A64*, 112−122.
(41) Farrugia, L. J. *J. Appl. Crystallogr.* **1997**, *30*, 565.
(42) Puntigam, O.; Hajdok, I.; Nieger, M.; Niemeyer, M.; Strobel, S.; Gudat, D. *Z. Anorg. Allg. Chem.* **2011**, *637*, 988−994.
(43) Dashti-Mommertz, A.; Neumüller, B. *Z. Anorg. Allg. Chem.* **1999**, *625*, 954−960.
(44) Cappello, V.; Baumgartner, J.; Dransfeld, A.; Hassler, K. *Eur. J. Inorg. Chem.* **2006**, 4589−4599.
(45) Borisenko, K. B.; Rankin, D. W. H. *Dalton Trans.* **2005**, 2382−2387.
(46) Weisbarth, R.; Jansen, M. *Z. Kristallogr. New Cryst. Struct.* **2002**, *217*, 94.
(47) Decken, A.; Gill, E. D.; Bottomley, F. *Acta Crystallogr., Sect. E* **2004**, *E60*, o1935−o1936.
(48) Kosolapoff, G. M.; Watson, R. M. *J. Am. Chem. Soc.* **1951**, *73*, 5466−5467.
(49) Harwood, H. J.; Becker, M. L.; Smith, R. C. *J. Org. Chem.* **1967**, *32*, 3882−3885.
(50) Nycz, J. E. *Pol. J. Chem.* **2009**, *83*, 589−594.
(51) Hill, N. J.; Reeske, G.; Cowley, A. H. *Main Group Chem.* **2010**, *9*, 5−10.
(52) Gallacher, A. C.; Pinkerton, A. A. *Acta Crystallogr., Sect. C* **1993**, *49*, 1793−1796.
(53) Fuller, A. L.; Scott-Hayward, L.; Li, Y.; Bühl, M.; Slawin, A. M. Z.; Woollins, J. D. *J. Am. Chem. Soc.* **2010**, *132*, 5799−5802.
(54) Giffin, N. A.; Masuda, J. D. *Coord. Chem. Rev.* **2011**, *255*, 1342−1359.

(55) Simon, A.; Borrmann, H.; Craubner, H. *Phosphorous, Sulfur Relat. Elem.* **1987**, *30*, 507−510.
(56) Simon, A.; Borrmann, H.; Horakh, J. *Chem. Ber. /Recl.* **1997**, *130*, 1235−1240.
(57) Niecke, E.; Rueger, R.; Krebs, B. *Angew. Chem.* **1982**, *94*, 553−554.
(58) Riedel, R.; Hausen, H. D.; Fluck, E. *Angew. Chem.* **1985**, *97*, 1050.
(59) Fluck, E.; Riedel, R.; Hausen, H. D.; Heckmann, G. *Z. Anorg. Allg. Chem.* **1987**, *551*, 85−94.
(60) Schroedel, H. P.; Noeth, H.; Schmidt-Amelunxen, M.; Schoeller, W. W.; Schmidpeter, A. *Chem. Ber. /Recl.* **1997**, *130*, 1801−1805.
(61) Fox, A. R.; Wright, R. J.; Rivard, E.; Power, P. P. *Angew. Chem., Int. Ed.* **2005**, *44*, 7729−7733.
(62) Lapczuk-Krygier, A.; Baranowska, K.; Pikies, J. *Acta Crystallogr., Sect. E* **2008**, *64*, o2427.
(63) Schoeller, W. W.; Lerch, C. *Inorg. Chem.* **1983**, *22*, 2992−2998.